UNIVERSITY OF CALIFORNIA SAN DIEGO

Multiplier Theory in Control

A dissertation submitted in partial satisfaction of the
requirements for the degree
Doctor of Philosophy

in

Engineering Sciences (Mechanical Engineering)

by

Yilong Chen

Committee in charge:

Professor Mauricío de Oliveira, Chair
Professor Robert R. Bitmead
Professor Jorge Cortés
Professor J. William Helton
Professor Miroslav Kristic

2021

The dissertation of Yilong Chen is approved, and it is acceptable in quality and form for publication on microfilm and electronically.

University of California San Diego

2021

DEDICATION

To all the men, women, and cat I met along the road.

TABLE OF CONTENTS

LIST OF FIGURES

LIST OF TABLES

ACKNOWLEDGEMENTS

Professor Maurício de Oliveira is not only my doctoral advisor but also like a mentor to my life. He led me into the world of engineering, guided me through all the challenges, and developed my skills in scientific research. My gratitude is beyond words. The PhD experience at University of California San Diego and collaboration with Professor Maurício has changed my life. This dissertation would not be possible without his guidance and his famous saying: "Details, details, and details."

I would also like to express my thanks to the rest of committee members. To Professor Miroslav Kristic, for your brilliant lecture on nonlinear systems and Lyapunov analysis methods. To Professor Jorge Corté, for your guidance on nonlinear control and hybrid system theory. To Professor Robert Bitmead, for you inspirational teaching in signals, real analysis, state-space, and linear systems in MIMO. Also, for tolerating my ignorant questions and helping me understand the connections in linear system theory. To Professor J. William Helton, for your great work in H_∞ control and development of the software, NCAlgebra, which helped me a lot in non-commutative algebraic operations.

Chapter Acknowledgments

Chapter 3, in part is currently being prepared for submission for publication of the material. Chen, Yilong, and Mauricio C. de Oliveira, "Positive Realness and Loop-Transformations for Systems with Sector-Bounded Nonlinearities". The dissertation author was the primary investigator and author of this material.

Chapter 4, in full, is a reprint of the material as it appears in: Chen, Yilong, and Mauricio C. de Oliveira. "An Alternative Algorithm to the DK Iterations for Robust Control Design." IEEE Control Systems Letters 5.1 (2020): 115-120. The dissertation author was the primary investigator and author of this material.

Chapter 5, in full, is a reprint of the material as it appears in: Chen, Yilong, and Mauricio C. de Oliveira. "Revisiting Stability Analysis of Phase-Locked Loops with the Popov Stability

Criterion.“ IFAC Journal of Systems and Control, (Manuscript Number: IFACSC-D-21-00010). The dissertation author was the primary investigator and author of this material.

VITA

2014-2017	B. S. in Mechanical Engineering, University of California San Diego
2017-2021	Ph. D. in Engineering Sciences (Mechanical Engineering), University of California San Diego

ABSTRACT OF THE DISSERTATION

Multiplier Theory in Control

by

Yilong Chen

Doctor of Philosophy in Engineering Sciences (Mechanical Engineering)

University of California San Diego, 2021

Professor Mauricío de Oliveira, Chair

Multiplier techniques is a powerful analysis tool in analyzing the closed-loop interconnection between a linear time-invariant system in feedback with a memoryless nonlinearity that belongs to certain class. In the literature, this is also known as the Lur'e type of problem and absolutely stable if the closed-loop system is asymptotically stable for all nonlinearity in the class. Many physical systems can be modeled with this type of interconnection, such as actuator saturation control problem, Phase-Locked Loop (PLL) design, steering control in vehicles, or even uncertainties in robust control design. Then through the passivity theorem, conditions for the stability of closed-loop interconnection can be constructed based purely on its linear part. However, the passivity arguments involves the strict positive-realness of transfer functions,

which are inherently conservative and may produce undesired results. This conservatism can be mitigated with the use of multiplier in the loop to achieve better results. Popular class of multipliers, such as the Circle and Popov criterion, and class of Zames-Falb multipliers, are stated in frequency domain but can also be converted into time-domain formulations through tools such as, Linear Matrix Inequalities (LMIs), and Positive-real Lemma, also known as the Kalman-Yakubovich-Popov (KYP) lemma.

This dissertation contributes to the multiplier theory in the following way: 1) Chapter 2 will explore different choice of loop transformation and establishes new results on the equivalence between different transformed systems; 2) Chapter 4 analyzes the connection between robust and absolute stability and develops new algorithm for the synthesis of robust controller; 3) Chapter 5 revisits the design challenge in PLL design and establishes new results on PLL stability.

Chapter 1

Basics

1.1 Background

Many physical systems are naturally nonlinear but can often be separated into linear and nonlinear part. The investigation of the closed-loop stability as a feedback of the linear system and the nonlinear component has been widely studied in the 1960s. The problem of *absolute stability*, which is a study of the closed-loop stability of the linear system in feedback with an entire class of nonlinearity, is often referred as the Lur'e problem, as in Figure 1.1. For example, the phase-locked loop filter design, perhaps the most widely deployed control devices in modern days, can be modeled as a linear system in feedback with nonlinearity $\psi(y) = \sin(y)$ as in Figure 1.1. The nonlinearity in this case can be considered in the class of sector-bounded nonlinearity, $\psi \in (\alpha, 1)$ and the design objective is to minimize the lower bound of the sector, α, which is equivalent to maximize the phase that the PLL system can synchronize up to. There are more examples in the practical implementations, such as the well-studied actuator saturation control problem, where the nonlinearity in this case is the saturation. In vehicle steering problem where the angular velocity is proportional to the tangent of steering angle, the nonlinearity in this case becomes $\psi(y) = \tan(y)$.

The condition of absolute stability for the closed-loop interconnection can often be derived based only on the linear system of the connection because the nonlinearity belongs to a specific class. This decoupling between linear system and nonlinear component greatly simplified the problem and simple analysis condition can be constructed using passivity theorem and strictly positive-realness. However, since these conditions are naturally conservative, the multiplier techniques are often used to reduce such conservatism. The basic idea of multiplier approach is that by multiplying certain appropriate multiplies that belongs to a specific class, the "scaled" system can now satisfy the passivity theorem to reduce the conservatism comparing to that of original "non-scaled" system. The most well-known and generic multiplier class is perhaps the Zames-Falb class [ZF68], developed in the late 1960s. Other popular criterion such as the Popov and Circle criterion [Pop61] was developed earlier and led to intuitive graphical test. Many books were interested in these topics, such as [AG64] focused on the Popov criterion and the Lur'e stability method, and [DV09] discussed the input-output version of the mutliplier theory and relation with small-gain theorem. In the work [CHL12], the authors there discussed causal and non-causal multiplier, and techniques regarding factorization of non-causal multiplier to retrieve causality, which is used for the passivity theorem.

In this dissertation, we will make some contributions to the multiplier theory in control. We begin with a brief introduction to the multiplier theory and absolute stability problem formulation. In chapter 3, we introduce new theorem and results on the loop transformation, which is required to generalize the results to arbitrary sector (α, β). We discuss some necessities to use one transformation versus the other. And different choice of loop transformations can actually been proved to be equivalent, including stability condition if given multiplier that has non-negative real parts. Moreover, we provides theorems discussing the possibilities to further enlarge the sector size of the nonlinearity by examining the tangential point of the scaled system response in frequency domain. From there, one can infer whether there would be need to examine both transformation or not.

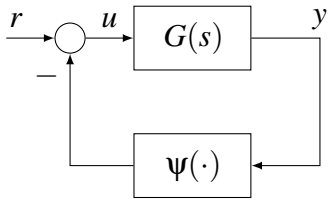

Figure 1.1: Interconnection of G and ψ.

Next, in chapter 4, we move on to discussing the connection between multiplier theory with robust control and small gain theorem. We provide new theorems to robust control design and formulate alternative algorithm to the traditional D-K iterations. The new algorithm is tested to perform better that the D-K iteration in the sense of both convergence time, and optimal value. The synthesize of the corresponding robust controller is also provided.

In chapter 5, we revisit the problem of phase-locked loop design using Popov/Circle criterion and utilizes the loop transformation theorem developed previously to construct new design techniques. In the literature, the coupling between parameters in stability and Popov criterion yields unnecessary iterative search for the optimal solution. We show that by utilize the other transformation, the solution will be find easily either through direct optimization or through graphical test. More to that, we also examine the properties of the PLL filter with order higher than three and provides concluding remarks and lemmas for that.

1.2 Notations

Notation is standard: $\mathbb{R}^{n\times m}$ denotes a n by m real matrix; the notation $X \succeq 0$ ($\preceq$) means that the symmetric real matrix X is positive (negative) semi-definite, and $X \succ 0$ ($\prec$) that X is positive (negative) definite. In certain symmetric block-matrices, the symbol ($\bullet$) is used to denote an entry that equals to its symmetric with respect to the main diagonal.

1.3 Memoryless Nonlinearties

1.3.1 Sector-Bounded Nonlinearties

A nonlinear function $\psi : \mathbb{R} \to \mathbb{R}$ is said to be in *sector* $[\alpha, \beta]$ or *sector-bounded* by $[\alpha, \beta]$, denoted $\psi \in [\alpha, \beta]$, if it satisfies

$$\alpha x^2 \leq \psi(x)\, x \leq \beta x^2, \qquad \forall x \in \mathbb{R}. \tag{1.1}$$

Note that the definition can be extended to multivariate case as follows.

Definition 1 (Multivariate Sector-bounded functions [KG02b])**.** *A memoryless function* $h : [0,\infty) \times \mathbb{R}^p \to \mathbb{R}^p$ *is said to belong to the sector*

1. $[0,\infty)$ *if* $u^T h(t,u) \geq 0$.
2. $[K_1,\infty)$ *if* $u^T (h(t,u) - K_1 u) \geq 0$.
3. $[0,K_2]$ *with* $K_2 = K_2^T > 0$ *if* $h^T(t,u)\,(h(t,u) - K_2 u) \leq 0$.
4. $[0,K_2]$ *with* $K_2 = K_2^T > 0$ *if* $h^T(t,u)\,(h(t,u) - K_2 u) \leq 0$.

In all cases, the inequality should hold for all (t,u)*. If in any case the inequality is strict, we write the sector as* $(0,\infty)$*,* (K_1,∞)*,* $(0,K_2)$*, or* (K_1,K_2)*.*

The above definitions admit a strict verision, in other words, $\psi \in (\alpha, \beta)$ if it satisfies,

$$\alpha x^2 < \psi(x) x < \beta x^2, \qquad \forall\, x \in \mathbb{R}.$$

1.3.2 Slope-Restricted Nonlinearties

The slope-restricted is defined as follows. The nonlinearty ψ is said to be slope-restricted or incrementally bounded in sector $[0,k]$, if

$$0 \leq \frac{\psi(x_1)-\psi(x_2)}{x_1-x_2} \leq k \tag{1.2}$$

for all $x_1 \neq x_2$.

Note that comparing to the slope-restricted class of nonlinearties, the sector-bounded nonlinearty is a harder class to work with because it does not constraint the derivative of the nonlinearity.

1.4 Passivity

One common tool in analyzing the Lur'e problem is the passivity theorem. Instead of analyzing the feedback interconnection as a whole, it decouples the linear and nonlinear part of the connection, which simplifies the problem and allows one to construct conditions based only on the linear part of the system interconnection. Furthermore, the passivity approach guarantees closed-loop stability for an entire class of nonlinearities, such as the class of sector-bounded, or the slope-restricted.

The following version of passivity theorem is from [CHL12].

Theorem 1 (Passivity Theorem)**.** *Let G be a stable LTI system and let ψ be a bounded system from $\mathcal{L}_{2e}^m[0,\infty)$ to $\mathcal{L}_{2e}^m[0,\infty)$. Assume that the feedback interconnection of G and ψ is well-posed and there exists a constant $\varepsilon > 0$ such that the following conditions hold*

$$< u, Gu > \geq \varepsilon \|u\|^2, \tag{1.3}$$

$$< u, \psi u > \geq 0, \tag{1.4}$$

for all $T > 0$ and $u \in \mathcal{L}_{2e}^m[0,\infty)$. Then, the feedback interconnection (2.4) *is stable.*

The passivity lemma provides a path in analyzing the absolute stability of the Lur'e problem by bounding the nonlineartiy term and solving the problem with SPR conditions. However, the passivity theorem admits conservatism. This can be reduced through an multiplier approach.

Theorem 2 (Passivity Theorem)**.** *Let G be a stable LTI system and let ψ be a bounded system from $\mathcal{L}_{2e}^m[0,\infty)$ to $\mathcal{L}_{2e}^m[0,\infty)$. Assume that the feedback interconnection of G and ψ is well-posed and there exists a constant $\varepsilon > 0$ and LTI multiplier M, such that $M(s)$ has a canonical factorization the following conditions hold*

$$< u, MGu > \geq \varepsilon \|u\|^2, \tag{1.5}$$

$$< u, M^* \psi u > \geq 0, \tag{1.6}$$

for all $T > 0$ and $u \in \mathcal{L}_{2e}^m[0,\infty)$. Then, the feedback interconnection (2.4) *is stable.*

1.5 Canonical Factorization

The factorization condition on the multiplier is given by

$$M = M_- M_+$$

where M_- and M_+ are invertible and stable with stable inverse. Factorization is widely used in the literature, [BGKR11] provides conditions on the existence of such factorization.

Definition 2 (Canonical Factorization [CHL12])**.** *Let $M(s)$ be a square matrix transfer function such that $M(s) \in \mathcal{RL}_\infty$ and $M^{-1}(s) \in \mathcal{RL}\infty$. Then, $M(s) = M_-(s)M_+(s)$ is a canonical factorization of $M(s)$ if $M_+(s) \in \mathcal{RH}_\infty$, $M_+(s) \in \mathcal{RH}_\infty$, $M_-^*(s) \in \mathcal{RH}_\infty$, and $(M_-^*(s))^{-1} \in \mathcal{RH}_\infty$*

1.6 Linear Matrix Inequalities

Modern control problems often involve using Linear Matrix Inequaility (LMIs) to efficiently guarantee stability or optimize performance. The notation and definition are standard, mainly from [BEGFB94].

A LMI has the form

$$F(x) \doteq F_0 + \sum_{i=1}^{m} x_i F_i \succ 0, \tag{1.7}$$

where $x \in \mathbb{R}^m$, and $F_i = F_i^T \in \mathbb{R}^{n \times n}$. The inequality (1.7) implies that $F(x)$ is positive definite, in other words,

$$u^T F(x) u > 0, \qquad \forall u \in \mathbb{R}^T.$$

In many control problems, the variables are matrices [BEGFB94], e.g., the Lyapunov inequality

$$A^T P + PA \prec 0, \tag{1.8}$$

where $A \in \mathbb{R}^{n \times n}$ is given and P is a variable. The phrase "the LMI $A^T P + PA \prec 0$ in P" means that the matrix P is a variable. Instead of the notation in (1.7), we will continue with this condensed form.

1.6.1 Convexity

A set C is convex if

$$\alpha x + (1 - \alpha) x \in C$$

for all $x \in C$ and $\alpha \in [0,1]$. An important property of LMIs is that the set $x : \quad F(x) > 0$ is convex. This enable use to solve control problem using the LMI and convex optimization approach.

1.6.2 Congruence Transformation

A transformation of the form $T^T F(x) T$ is known as the congruence transformation. One important property is that if $F(x) \succ 0$, then

$$T^T F(x) T \succ 0$$

provided that T is nonsingular.

1.7 Positive-Realness

In the next chapter, the stability of the feedback interconnection for the Lur'e problem lies heavily on the analysis whether one expression is strictly positive-real or not. In this section, we shall present the definition of SPR transfer function and important results on positive-realness.

Definition 3 (Positive-Real Transfer Function [KG02b])**.** *A $p \times p$ proper rational transfer function matrix $G(s)$ is called positive real if*

1. *poles of all elements of $G(s)$ are in* $\mathrm{Re}\{s\} \leq 0$*,*
2. *for all real ω for which $j\omega$ is not a pole of any element of $G(s)$, the matrix $G(j\omega) + G^T(-j\omega)$ is positive semidefinite, and*
3. *any pure imaginary pole $j\omega$ of any element of $G(s)$ is a simple pole and the residue matrix $\lim_{s \to j\omega} G(s)$ is positive semidefinite Hermitian.*

The transfer function $G(s)$ is called strictly positive-real *if $G(s-\varepsilon)$ is positive real for some $\varepsilon > 0$.*

Lemma 1 (Positive-Real [KG02b]). *Let $G(s) = C(sI - A)^{-1}B + D$ be a $p \times p$ transfer function matrix where (A,B) is controllable and (A,C) is observable. Then, $G(s)$ is positive-real if and only if there exist matrices $P = P^T > 0$, L, and W such that*

$$PA + A^T P = -L^T L, \tag{1.9}$$

$$PB = C^T - L^T W, \tag{1.10}$$

$$W^T W = D + D^T. \tag{1.11}$$

Proof. See [KG02b, Lemma 6.2] for proof. □

Lemma 2 (Kalman-Yakubovich-Popov [KG02b]). *Let $G(s) = C(sI - A)^{-1}B + D$ be a $p \times p$ transfer function matrix where (A,B) is controllable and (A,C) is observable. Then, $G(s)$ is strictly positive-real if and only if there exist matrices $P = P^T > 0$, L, and W, and a positive constant ε such that*

$$PA + A^T P = -L^T L - \varepsilon P, \tag{1.12}$$

$$PB = C^T - L^T W, \tag{1.13}$$

$$W^T W = D + D^T. \tag{1.14}$$

Proof. See [KG02b, Lemma 6.3] for proof. □

1.8 Bounded-real and Positive-real

The bounded-real and positive-real lemmas are useful tool in the robust control and multiplier problems. Here we shall present the results.

Let $A \in \mathbb{R}^{n\times n}$, $B \in \mathbb{R}^{n\times p}$, $C \in \mathbb{R}^{p\times n}$, and $D \in \mathbb{R}^{p\times p}$ be state space realization of a transfer

function $G(s)$. Assume that A is Hurwitz.

$$G: \begin{cases} \dot{x} & = \text{A x + B u}, \\ y & = \text{C x + D u}, \end{cases} \qquad x(0) = 0$$

1.8.1 Positive-real results

The followings are equivalent [Pap]:

1. The system $y = Gu$ is passive,

$$\int_0^T u(t)^T y(t) d\, t \geq 0,$$

for all u and $T \geq 0$.

2. The transfer function matrix $G(s) = C(sI - A)^{-1}B + D$ is bounded-real, which is

$$G^*(s) + G(s) \succ 0$$

for all s with $\text{Re}\{s\} > 0$

3. The LMI

$$\begin{bmatrix} A^T P + PA & PB - C^T \\ B^T P - C & -(D^T + D) \end{bmatrix} \prec 0,$$

in variable $P = P^T \succ 0$ is feasible.

4. There exists a real matrix $P = P^T \succ 0$ satisfying the algebraic riccati equation (ARE)

$$A^T P + PA + (PB - C^T)(D + D^T)^{-1}(PB - C^T)^T = 0$$

1.8.2 Bounded-real results

The followings are equivalent:

1. The system $y = Gu$ is nonexpansive,

$$\int_0^T y(t)^T y(t) d\, t \leq \int_0^T u(t)^T u(t) d\, t,$$

for all u and $T \geq 0$.

2. The transfer function matrix $G(s) = C(sI - A)^{-1}B + D$ is bounded real, which is

$$G^*(s)G(s) \prec I$$

for all s with $\mathrm{Re}\{s\} > 0$, or equivalently,

$$\|G(s)\|_\infty \leq 1.$$

3. The LMI

$$\begin{bmatrix} A^T P + PA + C^T C & PB + C^T D \\ B^T P + D^T C & D^T D - I \end{bmatrix} \prec 0,$$

in variable $P = P^T \succ 0$ is feasible.

4. There exists a real matrix $P = P^T \succ 0$ satisfying the algebraic riccati equation (ARE)

$$A^T P + PA + C^T C + (PB + C^T D)(I - D^T D)^{-1}(PB + C^T D)^T = 0$$

Chapter 2

Multiplier Theory

Recall that the Lur'e type of problem concerns with the absolute stability of a linear time-invariant system $G(s)$ with nonlinearity in a given class, such as sector-bounded in $(0,k)$, as shown in Figure 2.1.

The use of passivity or small-gain theorem decouples the linear system $G(s)$ and the nonlinearity ψ, from which simple conditions based only upon the linear system can be constructed and reduces the complexity of the problem. The conditions are often in the form of proving strictly positive-realness, which are naturally conservative. In order to reduce this natural conservatism, multiplier techniques can be used.

The multiplier is an artificial system, which, loosely speaking, examine the excess of positivity in the nonlinearity to mitigate the deficiency of positivity in the linear system [CHL12]. The multiplier is introduced into the loop along with its inverse, as shown in Figure 2.2, to retrieve of the original loop, as in Figure 2.1. Passivity theorem requires causality for the linear system, including the multiplier here. Such restriction tremendously limits the choice of potential multipliers by restraining the phase of the multiplier. This is overcome by a factorization on the non-causal multiplier in [ZF68] in order to recover causality in the loop, as shown in Figure 2.3.

With all these prepared, the multiplier theory utilizes the property of the positive nonlin-

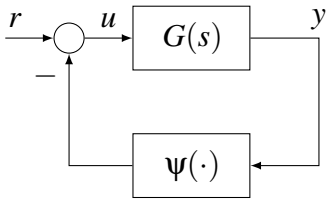

Figure 2.1: Interconnection of G and ψ.

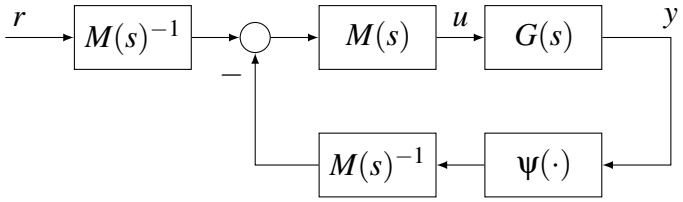

Figure 2.2: Interconnection with multiplier in loop.

earty ψ belonging to a given class Ψ and applies it to search for appropriate multiplier $M(s)$ in a certain class $\mathcal{M}$, which ensures the positivity of $M^*\psi$. For example, the famous Zames-Falb multiplier [ZF68] focuses on the class of monotone and slope-restricted nonlinearties. Then, with the help of passivitity theorem, the stability of the original feedback interconnection as in Figure 2.1 can be established if there exists a multiplier M within in a certain class such that

$$M(s)\left(\frac{1}{k}+G(s)\right)$$

is strictly positive-real (SPR).

The chapter will focus on the nonlinearity either sector-bounded or slope-restricted in sector $(0,k)$. First we will properly define the absolute stability and input-output stability, i.e., $\mathcal{L}_2$ stability. Then, we shall introduce popular multiplier criteria, such as Circle, Popov criteria and Zames-Falb multipliers. We shall discuss their advantages and disadvantages. Chapter 3 will generalize the results into arbitrary sector (α,β) via loop transformations and discusses intriguing observations.

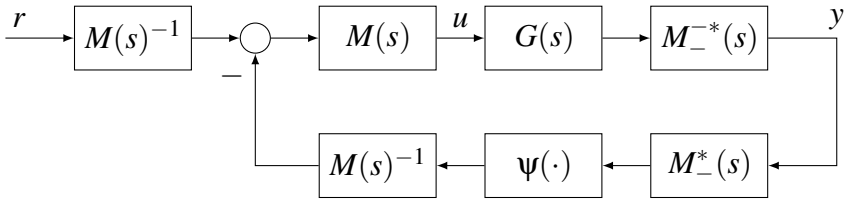

Figure 2.3: Interconnection with multiplier in loop.

2.1 Absolute and $\mathcal{L}_2$ Stability

2.1.1 $\mathcal{L}_p$ Stability

The following definition is from [Vid02]

Definition 4. *Suppose R is a binary relation of $\mathcal{L}_{pe}$. Then R is said to be L_p-*stable *if*

$$(x,y) \in R, \qquad\qquad x \in \mathcal{L}_p \Rightarrow y \in \mathcal{L}_p.$$

*R is $\mathcal{L}_p$-*stable with finite gain *if it is $\mathcal{L}_p$-stable, and in addition there exists finite constant γ_p and b_p such that*

$$(x,y) \in R, \qquad\qquad x \in \mathcal{L}_p \Rightarrow \|y\|_p \leq \gamma_p \|x\|_p + b_p.$$

*R is $\mathcal{L}_p$-*stable with finite gain and zero bias *if it is $\mathcal{L}_p$-stable, and in addition there exists finite constant γ_p such that*

$$(x,y) \in R, \qquad\qquad x \in \mathcal{L}_p \Rightarrow \|y\|_p \leq \gamma_p \|x\|_p.$$

The definition of $\mathcal{L}_p$ stability essentially defines bounded-input bounded-output with a user-specified norm. Throughout this dissertation, $p = 2$, or ∞. The important point is that the finite constant γ_p is independent of x. We shall see more of this in next chapter, when the loop transformation theorem shows up.

2.1.2 Absolute stability

Consider the system interconnection of a linear time-invariant system G and a sector-bounded nonlinearity ψ,

$$y = Gu, \qquad u = r - \psi(y), \tag{2.1}$$

as in Figure 2.1. The nonlinearity ψ is said to be sector-bounded, denoted $\psi \in (\alpha, \beta)$, if

$$\alpha x^2 \leq \psi(x)x \leq \beta x^2, \qquad \beta \geq \alpha \qquad \forall x \in \mathbb{R}. \tag{2.2}$$

Definition 5 (Absolute Stability, [KG02b])**.** *Consider the system* (2.1)*, where* ψ *satisfies a sector condition. The system is* absolutely stable *if the origin is globally asymptotically stable for any nonlinearity in the given sector. It is absolutely stable with a finite domain if the origin is uniformly asymptotically stable.*

2.2 Popov/Circle Criterion

One popular absolute stability criterion is the Popov/Circle criterion. First, we shall introduce the criterion

Lemma 3 (Popov criterion [CHL13])**.** *Consider an asymptotically stable linear time-invariant system* $G(s)$ *and a sector-bounded nonlinearity* $\psi \in (0, k)$ *with the interconnection shown in Figure 2.1. If there exists* $\gamma \in \mathbb{R}$ *such that*

$$Z(s) = \frac{1}{k} + (1 + \gamma s)G(s) \tag{2.3}$$

is SPR, then the feedback interconnection (2.1) *is* $\mathcal{L}_2$ *stable.*

Remark 1. *Note that the version of Popov criterion stated in the above lemma can take in any*

$\gamma \in \mathbb{R}$. *When* $\gamma > 0$*, it is the standard Popov criterion. When* $\gamma < 0$*, as pointed out by [CHL13], it is the anti-causal version of Popov. When* $\gamma = 0$*, one retrieves the Circle criterion.*

Remark 2. *The class of Popov multiplier is characterized by* $M(s) = 1 + \gamma s$*. Note that the Popov multipliers are not proper. Instead, the Zames-Falb multiplier requires the multiplier to be proper.*

Remark 3. *The meaning of the interconnection being* $\mathcal{L}_2$ *is that* e *and* η *are in* $\mathcal{L}_2$ *whenever* u *and* $\dot{u}$ *are in* $\mathcal{L}_2$*.*

Remark 4. *The function in* (2.3) *is SPR if and only if the function in* (3.1) *SPR with the multiplier* $M(s) = 1 + \gamma s$*.*

2.2.1 Graphical Approach

One major reason for the popularity of the Popov/Circle criterion is its graphical feature. Note that

$$Z(s) = \frac{1}{k} + (1 + \gamma s) G(s)$$

being strictly positive-real is equivalent to

$$\mathrm{Re}\left\{ \frac{1}{k} + (1 + \gamma j\omega) \left(\mathrm{Re}\{G(j\omega)\} + j\,\mathrm{Im}\{G(j\omega)\} \right) \right\} > 0, \qquad \forall \omega \in \mathbb{R}.$$

Expand the expression to have

$$\frac{1}{k} + \mathrm{Re}\{G(j\omega)\} - \gamma\omega\,\mathrm{Im}\{G(j\omega)\} > 0, \qquad \forall \omega \in \mathbb{R}.$$

From which one can construct the so-called "Popov plot", by plotting $\mathrm{Re}\{G(j\omega)\}$ versus $\omega\,\mathrm{Im}\{G(j\omega)\}$. The criterion now becomes finding a "Popov line" that lies entirely to left of the curve $\mathrm{Re}\{G(j\omega)\}$ versus $\omega\,\mathrm{Im}\{G(j\omega)\}$. The slope of the Popov line equals $1/\gamma$ and the Popov

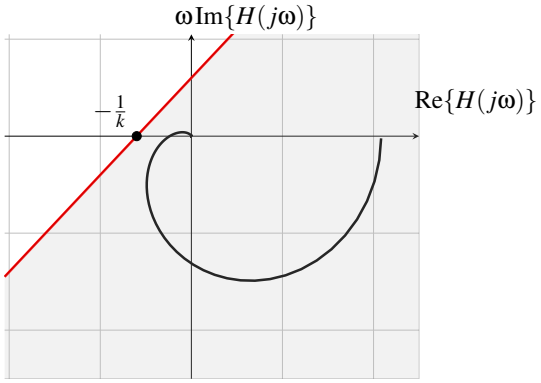

Figure 2.4: Popov plot. The curve is entirely lies to right of the red line that intersects the real axis at $-1/k + j0$ with a slope $\gamma^{-1} > 0$ such that (2.3) is SPR.

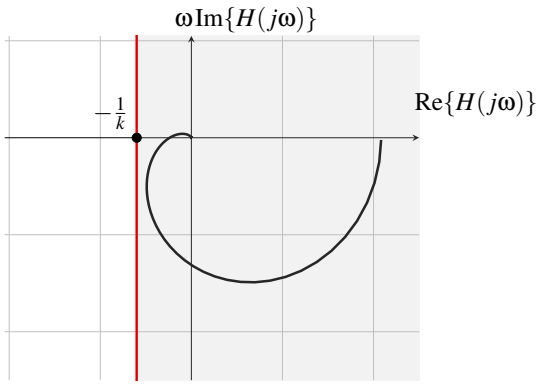

Figure 2.5: Recovery of Circle criterion with $\gamma = 0$.

line intercept the real axis at $-1/k + j0$. One example is shown in Figure 2.4 where $\gamma > 0$. The case of $\gamma = 0$ and $\gamma < 0$ are shown in Figure 2.5 and Figure 2.6, respectively.

2.2.2 Multivariate Popov

Consider a strictly-proper system

$$\dot{x} = Ax + Bu, \tag{2.4}$$

$$y = Cx, \tag{2.5}$$

$$u_i = -\psi_i(y_i),\ 1 \leq 1 \leq q, \tag{2.6}$$

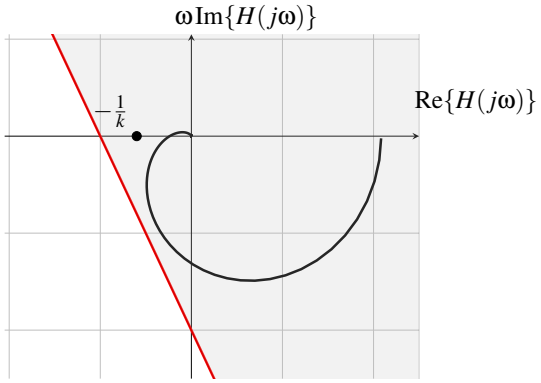

Figure 2.6: Popov plot with $\gamma < 0$.

where $A \in \mathbb{R}^{n\times n}$, $B \in \mathbb{R}^{n\times p}$, and $C \in \mathbb{R}^{p\times n}$, (A,B) is controllable, (A,C) is observable, and $\psi_i : \mathbb{R} \to \mathbb{R}$.

For the multi-input multi-output system, the Popov criterion can be stated as below

Lemma 4 (Multivariate Popov Criterion [KG02b])**.** *The system* (2.4) - (2.6) *is absolutely stable if, for* $1 \le i \le p$, $\psi_i \in (0,k_i)$, $0 < k_i < \infty$, *and there exists a constant* $\gamma_i \ge 0$, *with* $(1+\gamma_k\gamma_i) \neq 0$ *for every eigenvalue* λ_k *of A, such that*

$$Z(s) = M + (I + s\Gamma)G(s) \tag{2.7}$$

is strictly positive-real, where $\Gamma = \operatorname{diag}(\gamma_1,\ldots,\gamma_p)$ *and* $M = \operatorname{diag}(1/k_1,\ldots,1/k_p)$.

If the sector condition $\psi_i \in (0,k_i)$ *is satisfied only on a set* $Y \subset \mathbb{R}^p$, *then the foregoing conditions ensure that the system is absolutely stable with a finite domain.*

Proof. See [KG02b, Theorem 7.3] for proof. □

Remark 5. *Note that here the multiplier parameter matrix* Γ *is positive while the* γ *in Lemma 3 belongs to the entire real number set,* $\gamma \in \mathbb{R}$.

2.2.3 Popov LMI formulation

The multivariate formulation of the Popov criterion allows us to construct LMIs correspondents in the following process. Consider

$$Z(s) = M + (I + s\Gamma)C(sI - A)^{-1}B + D.$$

It is equivalent to

$$Z(s) = M + C(sI - A)^{-1}B + \Gamma sC(sI - A)^{-1}B.$$

Let $s = (sI - A + A)$, and expand the produce,

$$Z(s) = M + C(sI - A)^{-1}B + \Gamma CB + \Gamma CA(sI - A)^{-1}B.$$

Rearrange the terms,

$$Z(s) = (C + \Gamma CA)(sI - A)^{-1}B + M + \Gamma CB.$$

So the state-space realization of $Z(s)$ can be given as

$$Z : \begin{cases} \mathcal{A} = A, \\ \mathcal{B} = B, \\ \mathcal{C} = C + \Gamma CA, \\ \mathcal{D} = M + \Gamma CB. \end{cases}$$

From which one can utilizes the positive-real(KYP) lemma to have

$$\begin{bmatrix} P\mathcal{A}+\mathcal{A}^T P & \mathcal{C}^T - P\mathcal{B} \\ \mathcal{C}-\mathcal{B}^T P & -\mathcal{D}^T-\mathcal{D} \end{bmatrix} \prec 0$$

which leads to

$$\begin{bmatrix} PA+A^T P & (C+\Gamma CA)^T - PB \\ C+\Gamma C - B^T P & -(M+\Gamma CB)^T - (M+\Gamma CB) \end{bmatrix} \prec 0$$

2.3 Zames-Falb Criterion

The class of Zames-Falb multiplier is constructed in terms of monotone and slope-restricted nonlinearty instead of sector bounded. The Zames-Falb criterion is state as follows.

Lemma 5 (Zames-Falb criterion [CHL13])**.** *Consider the feedback system in Figure 2.1 with asymptotically stable $G(s)$ and a nonlinearity ψ slope-restricted in $(0,k)$. Assume that the feedback interconnection is well-posed. Then suppose that there exists a convolution operator $M : \mathcal{L}_2(-\infty,\infty) \to \mathcal{L}_2(-\infty,\infty)$ whose impulse response is of the form*

$$m(t) = \delta(t) - z_a(t) - \sum_i z_i \delta(t-t_i),$$

where δ is the Dirac delta function,

$$\sum_{i=0}^{\infty} |z_i| < \infty, \qquad\qquad z_a \in \mathcal{L}_1, \text{ and } t_i \in \mathbb{R}, \ \forall i \in \mathbb{N},$$

Assume that

1. $\|z_a\|_1 + \sum_i |z_i| < 1$.
2. *either $z_a(t) \geq 0$ for all $t \in \mathbb{R}$ and $z_i \geq 0$ for all $i \in \mathbb{N}$, or ψ is odd; and*

3. $\mathrm{Re}\{M(j\omega)(1+kG(j\omega))\} > 0, \quad \forall \omega \in \mathbb{R}.$

Then the feedback interconnection (2.1) *is* $\mathcal{L}_2$ *stable.*

Chapter 3

Equivalence Results in Loop Transformations

Loop transformation is often necessary in the Lur'e problem dealing with nonlinearty bounded by generic sector (α, β), as in Figure 3.1. Traditionally, the transformation utilizes the lower bound of sector, α. However, in many situations, this may complicates the problem unnecessarily due to coupling in parameters. This chapter explores the transformation using the upper bound β and establishes the relationships between the positive realness of the two transformed system. Then the equivalence result will be applied to popular absolute stability criteria involving positive realness, such as the Circle criterion, Popov and Zames-Falb multipliers.

Recall that in previous chapters, a sufficient condition to absolute stability of the closed-loop interconnection for a normalized nonlinearity is that

$$M(s)\left(\frac{1}{k}+H(s)\right) \tag{3.1}$$

is SPR, in which $H(s)$ is an asymptotically stable transfer-function obtained from $G(s)$ via a loop transformation. This is because most multiplier criteria, such as the Popov criterion (Lemma 3),

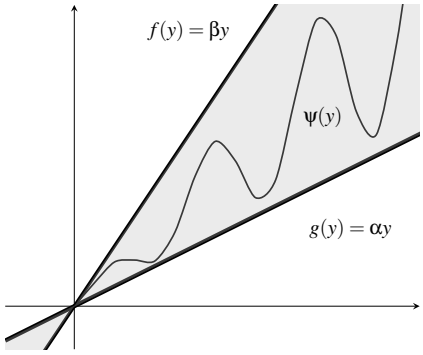

3.1(a) Sector (α, β), $\beta > \alpha$.

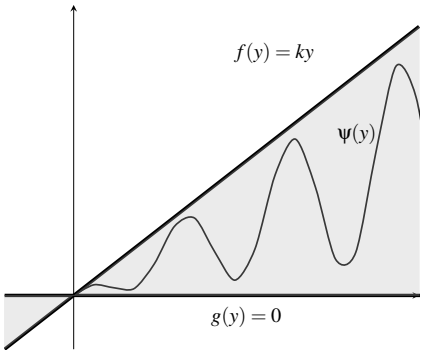

3.1(b) Sector $(0, k)$, $k > 0$.

Figure 3.1: Sector-bounded nonlinearities

requires the nonlinearity be in the normalized sector $(0, k)$. In order to deal with nonlinearities in a generic sector (α, β), a *loop transformation* is used to shift the sector from (α, β) to $(0, k)$.

Assume without loss of generality that $\beta > \alpha$. Traditionally, the loop transformation is performed by introducing feedback loops depending on the value of α as in Figure 3.23.2(a), which leads to a transformed system and sector nonlinearity of the form

$$G_\alpha(s) = \frac{G(s)}{1 + \alpha G(s)}, \qquad \psi_\alpha(y) = \psi(y) - \alpha y \in (0, \beta - \alpha). \tag{3.2}$$

If the transformed system, $G_\alpha(s)$, is asymptotically stable and

$$\frac{1}{\beta - \alpha} + (1 + \gamma s) G_\alpha(s)$$

is SPR, then Lemma 3 with $H(s) = G_\alpha(s)$ and $k = \beta - \alpha$ guarantees that the original interconnection is absolutely stable for all nonlinearities in the sector (α, β). Examples of the use of such a transformation in the literature are [Eva98, Ahm14, Abr02a, PDP85].

In many problems, the values of α or β might not be rigidly fixed, but could be further manipulated to maximize the size of the allowable sector, for instance by maximizing the value of $\beta - \alpha$. As one concrete application, one could use a sector nonlinearity to model vehicle steering.

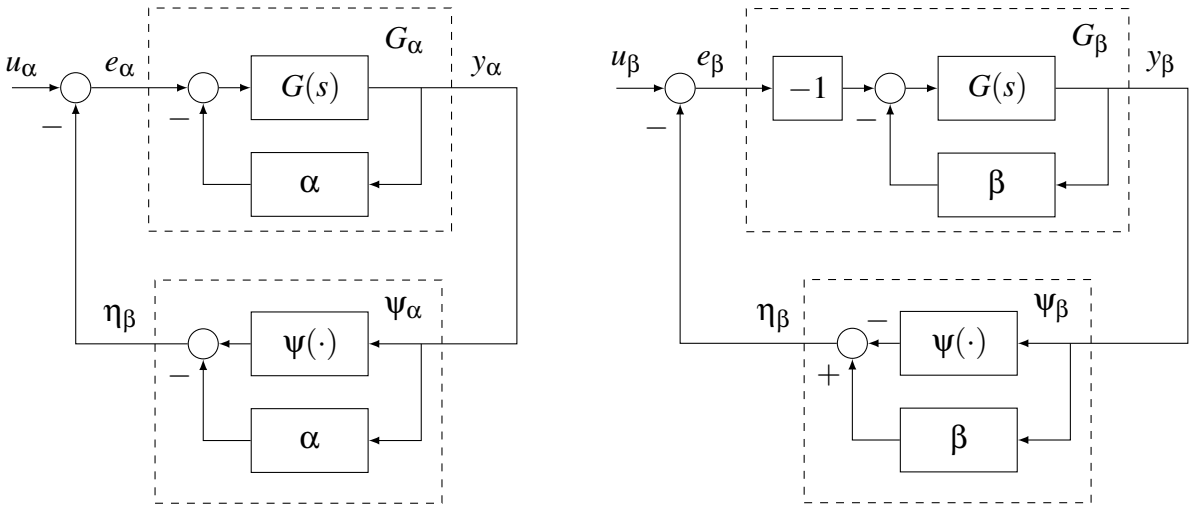

3.2(a) α loop transformation

3.2(b) β loop transformation

Figure 3.2: Loop transformations

Example 1 (Vehicle Steering)**.** *In the closed-loop control of a simplified model of a steering vehicle at constant forward velocity, the vehicle's angular velocity is proportional to the tangent of the steering angle, so that*

$$\dot{\theta} = \mu \tan(\theta), \qquad \phi = K(\bar{\theta} - \theta).$$

If $y = \theta$ *is bounded, then* $\tan(y) \in (\alpha, \beta)$*, in which* $\alpha = 1$ *and* β *is related to the maximum possible value of y, as shown in Figure 3.3. Stability of the closed-loop system can therefore be assessed by considering a transfer-function and the sector nonlinearity*

$$G(s) = \frac{\mu K}{s}, \qquad \psi(y) \in (1, \beta), \quad \beta > 1.$$

Using the loop transformation (3.2)*, one can shift the sector from* $(1, \beta)$ *to* $(0, k)$*,* $k = \beta - 1$*. The Popov criterion would be satisfied if there exists a* $\gamma \geq 0$ *such that* (2.3) *with*

$$H(s) = G_1(s) = \frac{G(s)}{1 + G(s)} \tag{3.3}$$

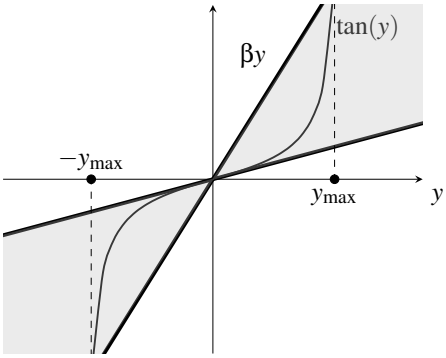

Figure 3.3: Vehicle steering nonliearity $\tan(y) \in (1, \beta)$. The maximum steering angle is denoted $y_{\max}$.

is SPR. Graphically, the Popov plot of G_1 *needs to lie to the right of the line that intercepts the point* $1/k + j0$ *with a slope* γ^{-1}*. Since the value of* $\alpha = 1$ *is fixed, the maximum possible* $k = \beta - 1$ *can be directly obtained from the Popov plot as the largest possible intercept* $-1/k + j0$*.*

In the vehicle steering example, the lower bound of the nonlinearity sector is constant, which makes maximizing the value of the upper bound very simple on the Popov plot. This feature is lost if the lower bound of the sector is what one needs to manipulate, as in the next examples.

Example 2 (Phase-locked Loop (PLL))**.** *The stability of* Phase-Locked Loops *(PLLs), perhaps the world's most widely deployed feedback system [Gar05, HH96, Jov03, Wu02b], has been analyzed by establishing absolute stability of the feedback interconnection of the system loop transfer function* $G(s) = s^{-1}L(s)$ *with a sine nonlinearity, which is contained in the sector* $(\alpha, 1),\ 1 > \alpha > 0$*, as in Figure 3.4 [Wu02b]. Other types of nonlinearities used with PLL can also be represented by sectors. Note that in this setup it is the lower bound, which corresponds to the PLL locking range [Wu02b], that needs to be minimized. In [Wu02b], the sector* $(\alpha, 1)$ *is shifted to* $(0, 1-\alpha)$ *using* (3.2) *and the Popov criterion is applied with*

$$H(s) = G_\alpha(s) = \frac{G(s)}{1 + \alpha G(s)}. \tag{3.4}$$

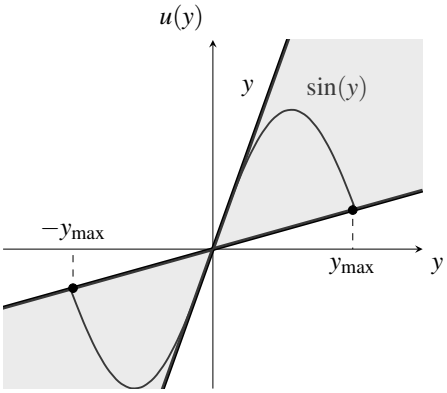

Figure 3.4: Sine nonliearity bounded by $(\alpha, 1)$ in the PLL problem. The maximum locking range is denoted by $y_{\max}$.

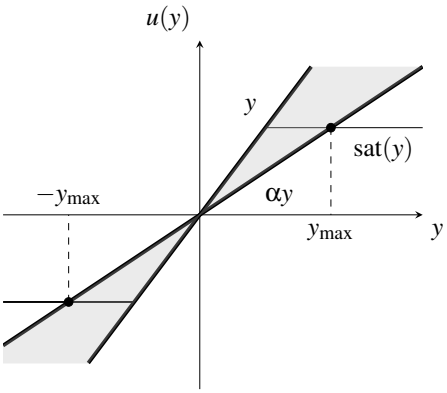

Figure 3.5: Saturation nonliearity

Note that now both the size of the sector, $k = 1 - \alpha$, as well as the transfer-function G_α depend on α. For this reason, one can no longer directly minimize the value of α by maximizing k in the Popov plot. The minimization has to be performed iteratively, which is further complicated by the need to ensure asymptotic stability of G_α.

Another example with a similar setup is the case of saturation nonlinearities.

Example 3 (Saturation nonlinearity)**.** *Control with input saturation is a widely-studied topic with many practical applications [TGdSJQ11, HL01, KG02a]. One popular approach is to model the saturation nonlinearity as a nonlinearity in the sector $(\alpha, 1)$ as shown in Figure 3.5. One would then proceed as in Example 2.*

In Examples 2 and 3, the dependence of $H(s) = G_\alpha(s)$ on the sector parameter α makes it impossible to directly minimize the parameter α in the Popov plot, as it was possible in the vehicle steering example. This difficulty can be overcome by using the alternative loop transformation

$$G_\beta(s) = \frac{-G(s)}{1+\beta G(s)}, \qquad \psi_\beta(y) = \beta y - \psi(y) \in (0, \beta - \alpha), \tag{3.5}$$

which is depicted in the block diagram shown in Figure 3.23.2(b). In this alternative setup, the transformed system $H(s) = G_\beta(s)$ no longer depends on α and, for a fixed β, α can again be directly optimized on the Popov plot.

Even though the alternative transformation (3.5) can be advantageous in several setups, it is rarely used in the literature. One reason for that might be that $H(s) = G_\beta(s)$ is often non-minimum phase even if $G(s)$ is minimum-phase. It is also not clear whether proving absolute stability using a certain criterion that holds for the transformation (3.2) would imply that the same absolute stability criterion holds for the alternative transformation (3.5). In fact, as shown later in the examples, it is possible, for instance, that the classical Popov criterion for a given sector $\psi \in (0, \beta - \alpha)$ holds for a system transformed using (3.2) but not for the same system transformed using (3.5), and vice-versa.

The rest of this chapter is dedicated to establishing relationships between absolute stability criteria applied to systems transformed using (3.2) or (3.5). Among other things, we show that proving absolute stability using one transformation is equivalent to proving absolute stability using the other transformation with the use of appropriate multipliers. One consequence of the new analysis, is an alternative proof for the existence of Popov multipliers without sign constraints, as first established in [CHL13]. Such equivalence relationships hold for the Circle criterion, the Popov criterion, and also for criteria using Zames-Falb multipliers [ZF68].

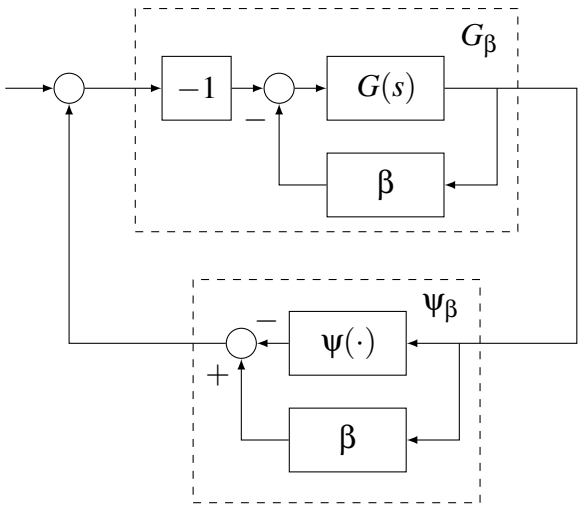

3.6(a) β loop transformation

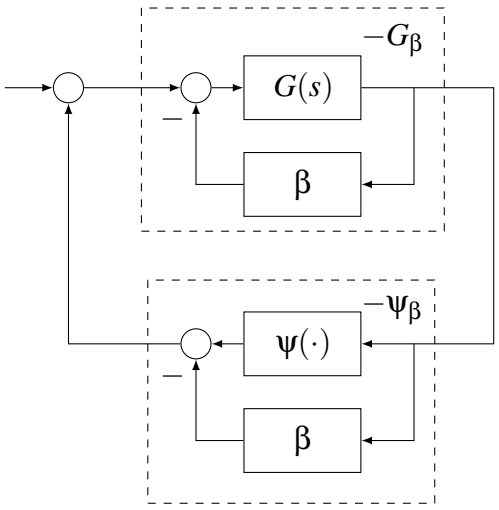

3.6(b) Equivalent α-type loop transformation

Figure 3.6: Loop transformations

3.1 Positive Realness with Loop Transformations and Multipliers

It is important to establish the equivalence between the stability of the original interconnection, Figure 2.1, and the α transformed loop, Figure 3.23.2(a), the β transformed loop, Figure 3.23.2(b), respectively. The α loop is standard in the literature for which [DV09, Theorem 6.3, Section III] proved that the feedback connection in Figure 2.1 is Bounded-Input Bounded-Output (BIBO) stable if and only if the feedback connection in Figure 3.23.2(a) is BIBO stable.

Observe that by by setting $\alpha = \beta$ and factoring out a -1 from the ψ_α block into the G_α block, one retrieves the β transformed loop, and vice versa. This equivalence between α and β transformed loop implies that the BIBO stability of β loop is also necessary and sufficient to the BIBO stability of the original interconnection.

The manipulation corresponds to first shift the generic sector (α, β) to $(\alpha - \beta, 0)$, and then

flip the sign of each interconnected blocks, shown as below.

$$\alpha y^2 < \psi(y)y < \beta y^2$$

Subtract βy^2 across all terms to obtain

$$(\alpha - \beta)y^2 < (\psi(y) - \beta y)y < 0.$$

Multiply -1 for all terms such that

$$0 < (\psi(y) - \beta y)y < (\beta - \alpha)y^2,$$

which is

$$0 < \psi_\beta(y)y < (\beta - \alpha)y^2.$$

The next theorem provides the key technical result relating the positive realness and asymptotic stability of the transfer-functions $G_\alpha(s)$ and $G_\beta(s)$ and a generic multiplier $M(s)$. This result will be further specialized to various absolute stability criteria in Section 3.2.

Theorem 3. *Let $G(s)$ and $M(s)$ be scalar functions with real coefficients and $\alpha, \beta \in \mathbb{R}$, $\beta > \alpha$, and let*

$$G_\alpha(s) = \frac{G(s)}{1 + \alpha G(s)}, \qquad G_\beta(s) = \frac{-G(s)}{1 + \beta G(s)}. \tag{3.6}$$

Assume that $\mathrm{Re}\{M(j\omega)\} \geq 0$ for all $\omega \in \mathbb{R}$. The followings are equivalent:

i) $G_\alpha(s)$ *is causal and asymptotically stable and the function*

$$Z_\alpha(s) = M(s)\left(\frac{1}{\beta-\alpha} + G_\alpha(s)\right)$$

is SPR.

ii) $G_\beta(s)$ *is causal and asymptotically stable and the function*

$$Z_\beta(s) = M(-s)\left(\frac{1}{\beta-\alpha} + G_\beta(s)\right)$$

is SPR.

Proof. See appendix 3.4. □

Remark 6. *Even though i) and ii) are equivalent in frequency domain, they are in terms different system,* $G_\alpha(s)$ *and* $G_\beta(s)$*, which can be very different as illustrated with examples in Section 3.2 using Circle and Popov criterion.*

Remark 7. *As noted in [CHL12, CTH16], because the scaled identity is a member of the sector nonlinearity* (2.2)*, the most general admissible classes of multipliers that are able to prove stability of the interconnection in Figure 2.1 must at least satisfy the constraint* $\mathrm{Re}\{M(j\omega)\} \geq 0$ *for all* $\omega \in \mathbb{R}$*.*

3.2 Applications

Theorem 3 connects the positive realness of the functions $Z_\alpha(s)$ and $Z_\beta(s)$ but does not prove the absolute stability for the interconnection between G and ψ. For that, it is necessary to establish further properties of the underlying multiplier class. This section applies Theorem 3 to a number of popular absolute stability criteria found in the literature, such as the Circle, Popov and Zames-Falb criteria.

3.2.1 Circle Criterion

The Circle criterion applied to the transfer-function $G_\alpha(s)$ and the sector nonlinearity ψ_α leads to a condition of the form *i*) in Theorem 3 in which $M(s) = 1$. Likewise, the Circle criterion applied to the transfer-function $G_\beta(s)$ and the sector nonlinearity ψ_β leads to a condition of the form *ii*) in Theorem 3 in which $M(-s) = M(s) = 1$. Because $M(j\omega) = 1 > 0$ for all $\omega \in \mathbb{R}$, Theorem 3 implies that asymptotic stability of G_α is equivalent to asymptotic stability of G_β. In other words that both conditions are completely equivalent. A formal statement of this equivalence can be obtained as a particular case of Corollary 1 in the next subsection.

Graphically, it means that the polar plot of $G_\alpha(j\omega)$ and the polar plot of $G_\beta(j\omega)$, which can differ from each other significantly, be both bounded by the exact same vertical line passing through $-1/(\beta-\alpha)+j0$. This is illustrated by the next example.

Example 4. *Consider the following transfer-function and sector-bounded nonlinearity*

$$G(s) = \frac{1}{(s+2)(s+3)(s+4)}, \qquad \psi \in (\alpha, \beta).$$

and a constant multiplier $M(s) = 1$. Let the sector upper bound β be fixed, say $\beta = 70$. The corresponding polar plot of $G_\beta(s)$ is shown in Figure 3.73.7(a). One can verify that if

$$\frac{1}{\beta-\alpha} \geq \frac{3}{250}, \qquad \alpha \geq \beta - \frac{250}{3} = -\frac{40}{3},$$

then the polar plot of $G_\beta(s)$ is to the right of the vertical line $s = -1/(\beta-\alpha)+0j$. The same vertical line is to the left of the polar plot of $G_\alpha(s)$ for $\alpha = -40/3$ as shown in Figure 3.73.7(b). This is true even though $G_\alpha(s)$, $G_\beta(s)$, and their polar plots are completely different.

Another side effect of the equivalence provided by Theorem 3 is that, as illustrated in Figure 3.7, the smallest value of α for which the polar plot of $G_\beta(s)$ is to the right of the vertical passing through $-1/(\beta-\alpha)+j0$, say $\bar{\alpha}$, coincides with the largest value of β for which the polar

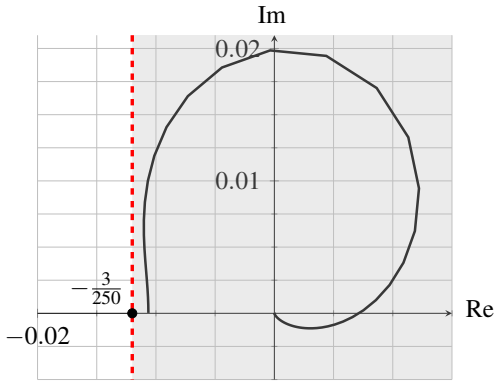

3.7(a) Polar plot of G_β, $\beta = 70$.

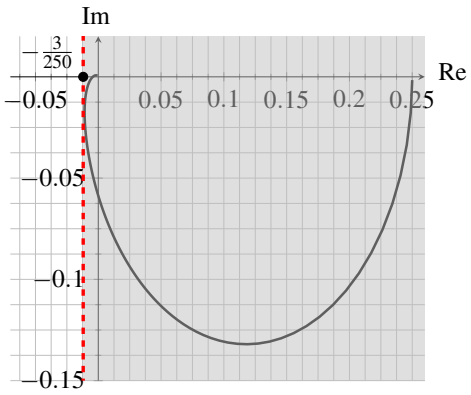

3.7(b) Polar plot of G_α, $\alpha = -20$.

Figure 3.7: Circle criterion, $M(s) = M(-s) = 1$.

plot and $G_{\bar{\alpha}}(s)$ is to the right of the vertical line $-1/(\beta - \bar{\alpha}) + j0$. This means that, in the case of circle criterion, one can not further optimize the sector size by iterating between the polas plots of $G_\alpha(s)$ and $G_\beta(s)$.

3.2.2 Popov Criterion

In this section, Theorem 3 will be applied to multipliers of the form $M(s) = 1 + \gamma s$, $\gamma > 0$, that is Popov multipliers. The next corollary follows from Theorem 3 and the Popov criterion from Lemma 3.

Corollary 1 (Application to Popov multipliers)**.** *Consider the single-input-single-output linear time-invariant system described by* (2.1)*, where* $\psi \in (\alpha, \beta)$*,* α*,* $\beta \in \mathbb{R}$*,* $\beta > \alpha$*, and* $G_\alpha(s)$*,* $G_\beta(s)$ *defined as in* (3.6)*, shown in Figure 3.23.2(a) and 3.23.2(b). Assume that for any* $u \in \mathcal{L}_2$*, e,* $\eta \in \mathcal{L}_2$*, as in Figure 2.1. The following statements are equivalent:*

i) Whenever u_α *and* $\dot{u}_\alpha \in \mathcal{L}_2$*,* e_α *and* η_α *are in* $\mathcal{L}_2$ *and there exists* $\gamma \in \mathbb{R}$ *such that*

$$Z_\alpha(s) = \frac{1}{\beta - \alpha} + (1 + \gamma s) G_\alpha(s)$$

is SPR.

ii) Whenever u_β and $\dot{u}_\beta \in \mathcal{L}_2$, e_β and η_β are in $\mathcal{L}_2$ and there exists $\gamma \in \mathbb{R}$ such that

$$Z_\beta(s) = \frac{1}{\beta - \alpha} + (1 - \gamma s) G_\beta(s)$$

is SPR.

Furthermore, if either i) or ii) is satisfied, then whenever u and $\dot{u} \in \mathcal{L}_2$, e and η are in $\mathcal{L}_2$.

Proof. Begin by noticing that $Z_\alpha(s)$ is SPR if and only if

$$\tilde{Z}_\alpha(s) = M(s)\left(\frac{1}{\beta - \alpha} + G_\alpha(s)\right), \qquad M(s) = 1 + \gamma s,$$

is SPR. Likewise, $Z_\beta(s)$ is SPR if and only if

$$\tilde{Z}_\beta(s) = M(-s)\left(\frac{1}{\beta - \alpha} + G_\beta(s)\right)$$

is SPR. Therefore, according to Theorem 3, $Z_\alpha(s)$ is SPR if and only if $Z_\beta(s)$ is SPR. Moreover, because $\mathrm{Re}\{M(j\omega)\} = \mathrm{Re}\{1 + j\gamma\omega\} = 1 > 0$, $G_\alpha(s)$ is asymptotically stable if and only if $G_\beta(s)$ is asymptotically stable, which proves the equivalence between items *i)* and *ii)*.

Concerning absolute stability of the interconnection, note that statement *i)* with $\gamma \geq 0$ is exactly the Popov criterion, which means that statement *ii)* with $\gamma \geq 0$ implies absolute stability of the interconnection via Theorem 3. Likewise, statement *ii)* with $\gamma \leq 0$ is also in the form of the Popov criterion, which this time means that statement *i)* with $\gamma \leq 0$ implies absolute stability of the interconnection via Theorem 3. □

Remark 8. *Theorem 3 also guarantees that the same value of parameter γ can be used in both statements i) and ii) of Corollary 1.*

Remark 9. *Corollary 1 includes the Circle criterion as the particular case $\gamma = 0$.*

Remark 10. *Note that since $G_\alpha(s)$ and $G_\beta(s)$ are asymptotically stable, $Z_\alpha(s)$ is strictly positive real if and only if*

$$\frac{1}{\beta-\alpha}+\mathrm{Re}\{G_\alpha(j\omega)\}-\gamma\omega\,\mathrm{Im}\{G_\alpha(j\omega)\}>0, \qquad \forall\omega\in\mathbb{R}, \tag{3.7}$$

whereas $Z_\beta(s)$ is strictly positive real if and only if

$$\frac{1}{\beta-\alpha}+\mathrm{Re}\{G_\beta(j\omega)\}+\gamma\omega\,\mathrm{Im}\{G_\beta(j\omega)\}>0, \qquad \forall\omega\in\mathbb{R}. \tag{3.8}$$

If $\gamma\neq 0$, then condition i) can be checked graphically on a Popov plot *by ensuring that the Popov curve of $G_\alpha(j\omega)$ lies to the right of the line that intercepts the point $-1/(\beta-\alpha)+j0$ with slope $\gamma^{-1}\neq 0$. If $\gamma>0$, then this is a standard Popov plot. Condition ii), requires that the Popov curve of $G_\beta(s)$ lies to the right of the line that intercepts the point $-1/(\beta-\alpha)+j0$ with slope $-\gamma^{-1}\neq 0$. If $\gamma<0$, this is a standard Popov plot.*

Remark 11. *Corollary 1 utilizes the most generic Popov criterion, that $\gamma\in\mathbb{R}$, instead of the classic Popov where $\gamma>0$. Note that in this dissertation, the proof to the generic Popov criterion only uses the classic Popov criterion and Theorem 3. However, this is not the case in the literature where the proof requires construction of Lyapunov functions.*

When the nonlinearities are slope-restricted instead of sector bounded, a similar condition was introduced in [CHL13], which was proved through an equivalence with Zames-Falb multipliers. See [CHL13, Lemma 4.5] for details.

The next examples illustrate the application of Corollary 1.

3.2.3 Zames-Falb Multipliers

In this section, Theorem 3 is applied to Zames-Falb multipliers [ZF68], which are defined next.

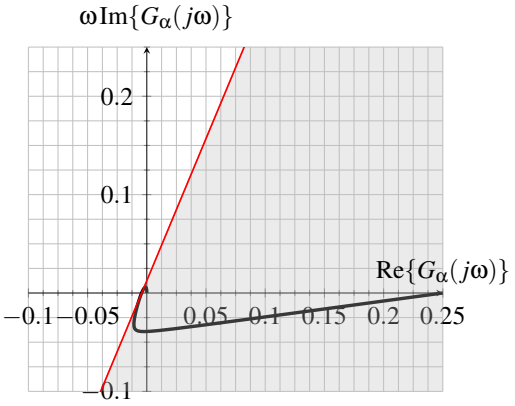

3.8(a) Popov plot of $G_\alpha(s)$, $\alpha = -20$, indicated by the black contour. The Popov line, with red color, has a slope of $\gamma^{-1} = 26/9$, and intersects the horizontal axis at $(-1/230, 0)$

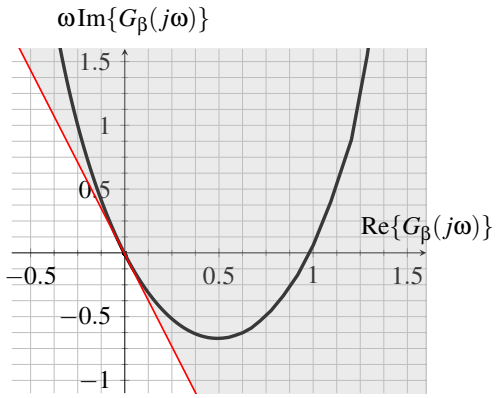

3.8(b) Popov plot of $G_\beta(s), \beta = 209$, indicated with black color. The red Popov line here has slope $-\gamma^{-1} = -26/9$ with the same intersection point as in (a).

Proposition 1. *The class of Zames-Falb multipliers $\mathcal{M}$ is given by all convolution operator $M : \mathcal{L}_2(-\infty,\infty) \to \mathcal{L}_2(-\infty,\infty)$ whose impulse response is of the form*

$$m(t) = \delta(t) - z_a(t) - \sum_i z_i \delta(t - t_i),$$

where δ is the Dirac delta function,

$$\sum_{i=0}^{\infty} |z_i| < \infty, \qquad\qquad z_a \in \mathcal{L}_1, \text{ and } t_i \in \mathbb{R}, \ \forall i \in \mathbb{N},$$

and

$$\|z_a\|_1 + \sum_i |z_i| < 1.$$

Furthermore, $M(s) = \mathcal{L}\{m(t)\}$, in which $\mathcal{L}\{\cdot\}$ is the bilateral Laplace transform, is such that

$$\mathrm{Re}\{M(j\omega)\} > 0, \quad \forall \omega \in \mathbb{R}.$$

In the above proposition, the definition of the Zames-Falb multipliers is from [ZF68,

CHL13] and the fact that the real part of $M(j\omega)$ is positive is proved in [CHLL12, SK00].

The Zames-Falb multipliers deals with monotone and slope-restricted nonlinearity, in which the definition is below

$$\alpha < \frac{\psi(x_1) - \psi(x_2)}{x_1 - x_2} < \beta, \tag{3.9}$$

or, in other words, ψ is slope-restricted in sector (α, β).

Note that the previous α, and β transformation in (3.2) and (3.5) work not only for sector-bounded nonlinearties in (2.2) but also the slope-restricted nonlinearties in (3.9). For α transformation in (3.2), it follows that

$$\alpha < \frac{(\psi(x_1) - \alpha x_1) - (\psi(x_2) - \alpha x_2) + \alpha x_1 - \alpha x_2}{x_1 - x_2} < \beta.$$

After rearranging and substituting ψ_α, one has

$$\alpha < \frac{\psi_\alpha(x_1) - \psi_\alpha(x_2)}{x_1 - x_2} + \alpha < \beta.$$

Subtract α on all parts of the inequality to obtain

$$0 < \frac{\psi_\alpha(x_1) - \psi_\alpha(x_2)}{x_1 - x_2} < \beta - \alpha,$$

which proves that the α transformation works with slope-restricted nonlinearties. Similarly, for β transformation in (3.5), follows the same procedure to obtain

$$\alpha < -\frac{\psi_\beta(x_1) - \psi_\beta(x_2)}{x_1 - x_2} + \beta < \beta.$$

After subtract β and multiply -1 through all, one has

$$0 < \frac{\psi_\beta(x_1) - \psi_\beta x_2}{x_1 - x_2} < \beta - \alpha, \tag{3.10}$$

which proves that the β transformation is also valid for slope-restricted nonlinearties.

The next corollary follows from applying Theorem 3 to the Zames-Falb criterion in [ZF68].

Corollary 2 (Application to Zames-Falb multipliers)**.** *Consider a linear time-invariant system $G(s)$ with a sloped-restricted nonlinearity $\psi(\cdot) \in (\alpha, \beta)$, $\alpha, \beta \in \mathbb{R}$, $\beta > \alpha$, $M(s) \in \mathcal{M}$ and $G_\alpha(s)$, $G_\beta(s)$ defined as in* (3.6)*. The following statements are equivalent:*

i) $G_\alpha(s)$ is asymptotically stable and

$$Z_\alpha(s) = M(s)\left(\frac{1}{\beta - \alpha} + G_\alpha(s)\right)$$

is SPR.

ii) $G_\beta(s)$ is asymptotically stable and

$$Z_\beta(s) = M(-s)\left(\frac{1}{\beta - \alpha} + G_\beta(s)\right)$$

is SPR.

Furthermore, if any of the above statement is satisfied, then the feedback interconnection (2.1) *is $\mathcal{L}_2$ stable.*

Proof. Equivalence between the two statements follows from Theorem 3 and the fact that $\mathrm{Re}\{M(j\omega)\} > 0$, for all $\omega \in \mathbb{R}$, from Proposition 1 and [CHLL12, SK00]. That both conditions satisfy the Zames-Falb criterion [ZF68] follows from the fact that $M(s) \in \mathcal{M}$ if and only if $M(-s) \in \mathcal{M}$, since $M(-s)$ corresponds to a time-reversal of impulse response $M(s)$ as a consequence of the time-reversal property of the bilateral Laplace transform [OV15]. □

Remark 12. *Neither $M(s)$ nor $G(s)$ is required to be rational in Corollary 2.*

The next example illustrates a concrete application of Corollary 2.

Example 5. *Consider*

$$G(s) = \frac{-(s+0.01)(s^2+0.6s+0.09)}{(s+0.8)^2(s^2+0.4s+0.04)}, \qquad \psi \in (\alpha, \beta).$$

and let $\alpha = -5$. One can verify that the Popov criterion is satisfied for any β such that

$$\beta - \alpha < 5.$$

Now consider a first-order Zames-Falb rational multiplier, which is a transfer-functions of the form [CHL13, Corollary 4.3]

$$M(s) = \frac{1+\nu s}{1+\kappa s}, \qquad \nu\kappa > 0, \qquad \left|1 - \frac{\nu}{\kappa}\right| < \frac{\nu}{\kappa}.$$

As expected, $M(-s)$ also satisfy the above constraints. One can verify that if

$$\nu = -\frac{17}{3}, \qquad \kappa = -83,$$

then condition i) in Corollary 2 is satisfied for all β such that

$$\beta - \alpha < 5.25.$$

This can be visualized by plotting

$$\frac{-\mathrm{Re}\{M(j\omega)\}}{\mathrm{Re}\{M(j\omega)G_\alpha(j\omega))\}} > \beta - \alpha = 5.25 \tag{3.11}$$

in Figure 3.9. Conversely, one can verify that condition ii) in Corollary 2 is satisfied for $\beta = 0.25$

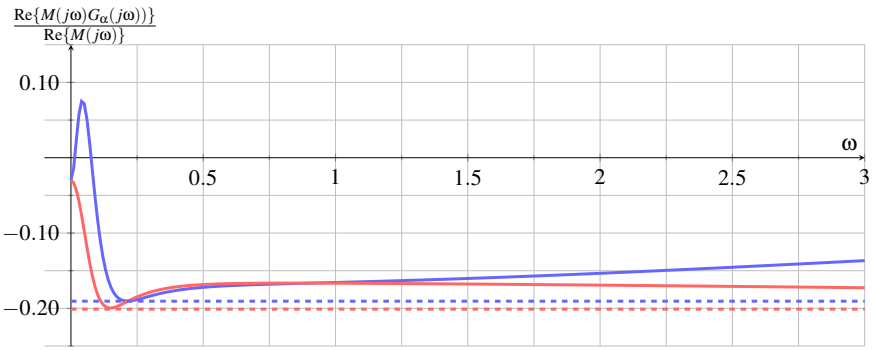

Figure 3.9: Plot of (3.11). Solid red and blue curve are LHS of (3.11) for Popov and Zames-Falb multiplier, respectively. The dashed red and blue line indicates their lowest bound, corresponding to the maximum sector size, $\beta - \alpha = 5$ for Popov multiplier and $\beta - \alpha = 5.25$ for Zames-Falb multiplier.

and that

$$\frac{-\mathrm{Re}\{M(-j\omega)\}}{\mathrm{Re}\{M(-j\omega)G_\beta(j\omega))\}} > \beta - \alpha = 5.25. \tag{3.12}$$

A plot of (3.12) *and also the function corresponding to the Popov criterion are also plotted in Figure 3.9.*

3.3 Discussion

Theorem 3 shows that the SPR condition of the rarely used β transformed loop is equivalent to that of the popular α transformed loop. As illustrated with the Example 1, 2, and 3, proper choice of transformation method will simplify the unnecessary numerical calculations. Equation (3.9)-(3.10) also shows that the β transformation is valid for the class of slope-restricted nonlinearties, which is considered in the Zames-Falb criterion. Section 3.2 provides applications of the equivalence result in Theorem 3 to the popular absolute stability criteria in the literature Circle, Popov and the Zames-Falb multipliers.

It is worth pointing out that for the class of sector-bounded nonlinearties, the generic Popov criterion, including the negative Popov constant is proved using only the classic Popov

criterion and Theorem 3, whereas [CHL13] proves this result for the class of slope-restricted nonliearties via an equivalence with Zames-Falb multiplier. Furthermore, the classic Popov criterion [KG02c] was proved by constructing a Lyapunov function, which is only valid with positive Popov constant. It is thus worth exploring the underlying connection between the positive and negative Popov constants, in terms of LMIs.

3.4 Proof to Theorem 3

Direction $i) \rightarrow ii)$.

Assume that $G_\alpha(s)$ is asymptotically stable and that $Z_\alpha(s)$ is SPR, that is

$$\mathrm{Re}\left\{M(j\omega)\left(\frac{1}{\beta-\alpha}+G_\alpha(j\omega)\right)\right\}>0 \quad \text{for all } \omega\in\mathbb{R}. \tag{3.13}$$

Expanding (3.13),

$$\mathrm{Re}\{M(j\omega)\}\left(\frac{1}{\beta-\alpha}+\mathrm{Re}\{G_\alpha(j\omega)\}\right)-\mathrm{Im}\{M(j\omega)\}\,\mathrm{Im}\{G_\alpha(j\omega)\}>0, \qquad \forall\omega\in\mathbb{R}.$$

In particular

$$\mathrm{Re}\{M(j\omega)\}\left(\frac{1}{\beta-\alpha}+\mathrm{Re}\{G_\alpha(j\omega)\}\right)>0, \quad \text{for all } \omega \text{ such that } \mathrm{Im}\{G_\alpha(j\omega)\}=0,$$

which implies that

$$\mathrm{Re}\{M(j\omega)\}>0, \qquad \mathrm{Re}\{G_\alpha(j\omega)\}>-\frac{1}{\beta-\alpha}, \quad \text{for all } \omega \text{ such that } \mathrm{Im}\{G_\alpha(j\omega)\}=0.$$

because $\mathrm{Re}\{M(j\omega)\}\geq 0$ for all $\omega\in\mathbb{R}$. Furthermore, because $G_\alpha(s)$ does not have purely

imaginary poles, the Nyquist plot of $G_\alpha(s)$ never encircles the point $-1/(\beta-\alpha)+j0$ so that

$$1+(\beta-\alpha)G_\alpha(s)$$

has no zeros on the right hand side of the complex plane [DO17]. In other words, that the rational function

$$G_\beta(s)=\frac{1}{\beta-\alpha}\left(\frac{1}{1+(\beta-\alpha)G_\alpha(s)}-1\right)=\frac{-G_\alpha(s)}{1+(\beta-\alpha)G_\alpha(s)}$$

is asymptotically stable.

Now define

$$X_\alpha(j\omega)=(\beta-\alpha)\,\mathrm{Re}\{G_\alpha(j\omega)\},\qquad Y_\alpha(j\omega)=(\beta-\alpha)\,\mathrm{Im}\{G_\alpha(j\omega)\},$$

and rewrite inequality (3.13) as

$$\frac{1}{\beta-\alpha}\,\mathrm{Re}\,\{M(j\omega)(1+X_\alpha(j\omega)+jY_\alpha(j\omega))\}>0,$$

which is equivalent to,

$$\frac{1}{\beta-\alpha}\,\mathrm{Re}\,\{M(-j\omega)(1+X_\alpha(j\omega)-jY_\alpha(j\omega))\}>0 \tag{3.14}$$

after taking the complex conjugate and using the fact that $M(j\omega)^*=M(-j\omega)$. Note that the strictness of (3.14) implies $1+X_\alpha(j\omega)-jY_\alpha(j\omega)\neq 0$ such that

$$(1+X_\alpha(j\omega))^2+Y_\alpha(j\omega)^2=(1+X_\alpha(j\omega)+jY_\alpha(j\omega))(1+X_\alpha(j\omega)-jY_\alpha(j\omega))>0.$$

Divide (3.14) by the positive number $(1+X_\alpha(j\omega))^2+Y_\alpha(j\omega)^2$ to obtain

$$\frac{1}{\beta-\alpha}\mathrm{Re}\left\{M(-j\omega)\frac{1}{1+X_\alpha(j\omega)+jY_\alpha(j\omega)}\right\}=\frac{1}{\beta-\alpha}\mathrm{Re}\left\{M(-j\omega)\frac{1}{1+(\beta-\alpha)G_\alpha(j\omega)}\right\}>0.$$

Furthermore,

$$(1+(\beta-\alpha)G_\alpha(j\omega))(1+(\beta-\alpha)G_\beta(j\omega))=1 \tag{3.15}$$

because $G_\alpha(s)$ and $G_\beta(s)$ are asymptotically stable and have no purely imaginary poles. It is then possible to conclude that

$$\frac{1}{\beta-\alpha}\mathrm{Re}\left\{M(-j\omega)(1+(\beta-\alpha)G_\beta(j\omega))\right\}>0,$$

in other words, that

$$Z_\beta(s)=M(-s)\left(\frac{1}{\beta-\alpha}+G_\beta(s)\right)$$

is SPR.

Conversely, assume that $G_\beta(s)$ is asymptotically stable and that $Z_\beta(s)$ is SPR such that

$$\mathrm{Re}\left\{M(-j\omega)\left(\frac{1}{\beta-\alpha}+G_\beta(j\omega)\right)\right\}>0, \qquad \forall\omega\in\mathbb{R}. \tag{3.16}$$

Similarly,

$$\mathrm{Re}\{M(-j\omega)\}>0, \quad \mathrm{Re}\{G_\beta(j\omega)\}>-\frac{1}{\beta-\alpha}, \quad \text{for all } \omega \text{ such that } \mathrm{Im}\{G_\alpha(j\omega)\}=0,$$

because $\mathrm{Re}\{M(-j\omega)\}=\mathrm{Re}\{M(j\omega)\}\geq 0$ for all $\omega\in\mathbb{R}$. Since, $G_\beta(s)$ does not have purely imaginary poles, the Nyquist plot of $G_\beta(s)$ never encircles the point $-1/(\beta-\alpha)+j0$ such that

the rational function

$$G_\alpha(s) = \frac{1}{\beta-\alpha}\left(\frac{1}{1+(\beta-\alpha)G_\beta(s)} - 1\right) = \frac{-G_\beta(s)}{1+(\beta-\alpha)G_\beta(s)},$$

is asymptotically stable.

Follow the steps in direction $i) \rightarrow ii)$ to show that

$$\frac{1}{\beta-\alpha}\,\mathrm{Re}\left\{M(j\omega)\frac{1}{1+(\beta-\alpha)G_\beta(j\omega)}\right\} > 0.$$

Furthermore, using (3.15)

$$\frac{1}{\beta-\alpha}\,\mathrm{Re}\left\{M(j\omega)(1+(\beta-\alpha)G_\alpha(j\omega)\right\} > 0,$$

and

$$Z_\alpha(s) = M(s)\left(\frac{1}{\beta-\alpha} + G_\alpha(s)\right)$$

is SPR.

3.5 Acknowledgment

Chapter 3, in part is currently being prepared for submission for publication of the material. Chen, Yilong, and Mauricio C. de Oliveira, "Positive Realness and Loop-Transformations for Systems with Sector-Bounded Nonlinearities". The dissertation author was the primary investigator and author of this material.

Chapter 4

Multipliers for Robust Control

Robust control concerns with the closed-loop stability between a linear system and an uncertainty block. The establishment of robust stability often involves the famous Small-Gain Theorem. The configuration is similar to that in the multiplier and passivity setup. Moreover, the uncertainty block also admits to certain properties such that the closed-loop stability can be constructed based on the linear system alone. The Small-Gain Theorem utilizes the H_∞ norm of the feedback interconnection, and provides a sufficient condition for the closed-loop stability.

We shall see in the next sections that the small gain theorem is similar to the passivity theorem in some sense, as the comparison between bounded-real and positive-real results in section 1.8. Furthermore, multipliers will also be utilized here to reduce conservatism, which is naturally inherited in these theorems.

The difference between the robust control method and the multiplier criterion mainly lies in the goal. The multiplier criterion aims to analyze the feedback interconnection but does not provide any formulations of the practical controller. Instead, the robust control design focuses on the synthesize of controllers that can ”robustly” stabilize the closed-loop under uncertainties.

4.1 $\mathcal{L}_2/\mathcal{H}_2$ and $\mathcal{L}_\infty/\mathcal{H}_\infty$ Norms

This section will provide definition of $\mathcal{L}_2/\mathcal{H}_2$ and $\mathcal{L}_\infty/\mathcal{H}_\infty$ norms and important lemmas on computing them.

4.1.1 $\mathcal{L}_2/\mathcal{H}_2$ Norm

Let $G(s) \in \mathcal{L}_2$ and the $\mathcal{L}_2$ norm of $G(s)$ is defined as

$$\begin{aligned}\|G\|_2 &:= \left(\frac{1}{2\pi}\int_{-\infty}^{\infty} \text{trace}\{G^*(j\omega)G(j\omega)\}\, d\omega\right)^{1/2} \\ &= \left(\int_{-\infty}^{\infty} \text{trace}\{g^*(t)g(t)\}\, dt\right)^{1/2}\end{aligned}$$

where $g(t)$ denotes the convolution kernel of $G(s)$.

Lemma 6. *Consider a transfer function matrix*

$$G(s) = \begin{bmatrix} A & B \\ C & D \end{bmatrix} \in \mathbb{RL}_\infty$$

with A Hurwitz. Then we have

$$\|G\|_2^2 = \text{trace}(B^*QB) = \text{trace}(CpC^*)$$

where Q and P are observability and controllability Gramians that can by obtained from

$$AP + PA^* + BB^* = 0, \qquad A^*Q + QA + C^*C = 0.$$

4.1.2 $\mathcal{L}_\infty/\mathcal{H}_\infty$ Norm

Let $G(s) \in \mathbb{RL}_\infty$ and the $\mathcal{L}_\infty$ norm of a matrix rational transfer function $G(s)$ is defined as

$$\|G\|_\infty := \sup_\omega \bar{\sigma}\{G(j\omega)\}$$

For the scalar case, the infinity norm represents the distance between the farthest point and the origin on the Nyquist plot of G, or, the peak magnitude value on the Bode plot of G.

Lemma 7. *Let* $\gamma > 0$ *and*

$$G(s) = \begin{bmatrix} A & B \\ C & D \end{bmatrix} \in \mathbb{RL}_\infty$$

Then $\|G\|_\infty < \gamma$ *if and only if* $\bar{\sigma}(D) < \gamma$ *and the Hamiltonian matrix* H *has no eigenvalues on the imaginary axis where*

$$H := \begin{bmatrix} A + BR^{-1}D*C & BR^{-1}B^* \\ -C^*(I + DR^{-1}D^*)C & -(A + BR^{-1}D^*C)^* \end{bmatrix}$$

and $R = \gamma^2 I - D^*D$.

4.2 Uncertain, Robust stability, and Small Gain Theorem

The term *uncertainty* refer to the differences between the mathematical model and practical implementation. The mechanism to express such error and difference is called *uncertainty representation*, as we shall see in the next sections. There are various kinds of uncertainty structure. In this chapter, we limited our focus to the additive uncertainties and introduce the frequency-domain condition on the stability of the closed-loop interconnection using the so-called

small gain theorem.

Moreover, the uncertainty representation does not only apply to physical imperfections but can also be used to analyze and design for those nonlinear system that can be separated into linear and nonlinear part. As we shall see next, by assuming certain properties for the uncertainty/nonlinearity, one can conclude the closed-loop robust stability by establishing conditions on the linear part alone, both in frequency-domain and time-domain.

This is very similar to the multiplier criterion and concept of absolute stability. In the end of this chapter, we shall also discuss the similarity and discrepancy between the small gain theorem vs. passivity theorem, and robust stability and absolute stability.

4.2.1 Robust stability

The terminologies used in this chapter are mainly followed from [ZD98]

Definition 6. *Given the description of an uncertainty model set* Π *and a set of performance objectives, suppose* $P \in \Pi$ *is the nominal design model and K is the resulting controller. Then the closed-loop feedback system is said to have*

1. ***Nominal Stability:*** *if K internally stabilizes the nominal model P.*
2. ***Robust Stability:*** *if K internally stabilizes every plant belonging to* Π.
3. ***Nominal Performance:*** *if the performance objectives are satisfied for the nominal plant P.*
4. ***Robust Performance:*** *if the performance objectives are satisfied for every plant belonging to* Π.

4.2.2 Small Gain Theorem

Here we shall introduce the frequency-domain version of the small gain theorem. In the next sections, we will develop a time-domain correspondents of it using LMIs.

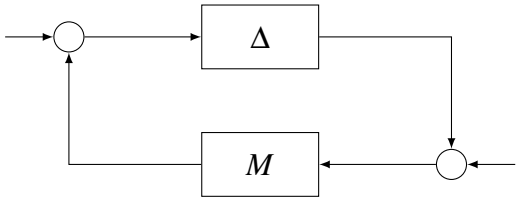

Figure 4.1

Theorem 4. *Suppose $M \in \mathbb{RH}_\infty$ and let $\gamma > 0$. Then the interconnected system shown in Figure 4.1 is well-posed and internally stable for all $\Delta(s) \in \mathbb{RH}_\infty$ with*

a) $\|\Delta\|_\infty < 1/\gamma$ *if and only if* $\|M(s)\|_\infty \leq \gamma$,

b) $\|\Delta\|_\infty < 1/\gamma$ *if and only if* $\|M(s)\|_\infty \leq \gamma$,

Proof. See [ZD98, Theorem 8.1] for proof. □

4.3 Linear Fractional Transformation

The definition of upper and lower linear fractional transformation is as follows

Definition 7. *Let M be a complex matrix partitioned as*

$$M = \begin{bmatrix} M_{11} & M_{12} \\ M_{21} & M_{22} \end{bmatrix} \in \mathbb{C}^{(p_1+p_2)\times(q_1+q_2)}$$

and let $\Delta_\ell \in \mathbb{C}^{q_2\times p_2}$ and $\Delta_u \in \mathbb{C}^{q_1\times p_1}$ be two other complex matrices. Then the lower LFT *with respect to Δ_ℓ as*

$$\mathcal{F}_\ell(M,\Delta_\ell) := M_{11} + M_{12}\Delta_\ell(I - M_{22}\Delta_\ell)^{-1}M_{21}$$

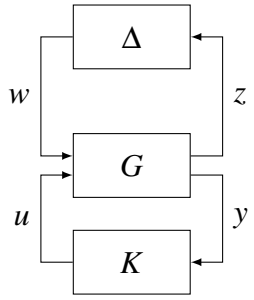

Figure 4.2: Closed loop H_∞ Configuration

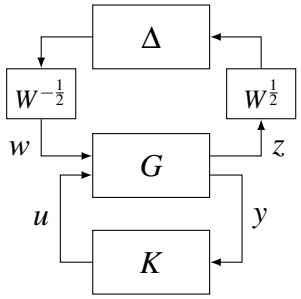

Figure 4.3: Closed loop H_∞ Configuration with multiplier.

provided that the inverse $(I - M_{22}\Delta_\ell)^{-1}$ *exists. The* upper LFT *with respect to* Δ_u *is*

$$\mathcal{F}_\ell(M, \Delta_\ell) := M_{22} + M_{21}\Delta_u(I - M_{11}\Delta_u)^{-1}M_{12}$$

provided that the inverse $(I - M_{22}\Delta_\ell)^{-1}$ *exists.*

We shall see these notations a lot in the next sections, when defining the H_∞ control problems and developing algorithms.

4.4 Problem Formulation

In this section we will formulate the problem through minimization on the H_∞ norm of the closed-loop interconnection and provides variants of the H_∞ theorem.

Consider a proper continuous-time linear time-invariant system G in feedback with controller K and interconnected with an uncertainty Δ as shown in Fig. 4.2.

Assume that G has minimal realization given by

$$\begin{bmatrix} \dot{x}(t) \\ z(t) \\ y(t) \end{bmatrix} = \begin{bmatrix} A & B_w & B_u \\ C_z & D_{zw} & D_{zu} \\ C_y & D_{yw} & D_{yu} \end{bmatrix} \begin{bmatrix} x(t) \\ w(t) \\ u(t) \end{bmatrix}, \tag{4.1}$$

in which $A \in \mathbb{R}^{n\times n}$, $B_u \in \mathbb{R}^{n\times m}$, $B_w \in \mathbb{R}^{n\times q}$, $C_z \in \mathbb{R}^{q\times n}$, $C_y \in \mathbb{R}^{p\times n}$, $D_{zw} \in \mathbb{R}^{q\times q}$, $D_{zu} \in \mathbb{R}^{q\times m}$, $D_{yw} \in \mathbb{R}^{n\times n}$, and that (A, B_u) is stabilizable, (A, C_y) is detectable, $D_{yu} = 0$, and, without loss of generality (see [AG95] for details), that G_{zw} and Δ are square. For simplicity, in the present chapter, we focus on an uncertainty Δ that is time-varying and block-diagonal with structure belonging to the following set

$$\begin{aligned} \mathcal{D}_\Delta = \{\Delta : \Delta = \operatorname{diag}(\delta_1 I_{q_1}, \ldots, \delta_\ell I_{q_\ell}, \Delta_1, \ldots, \Delta_s), \\ \delta_i \in \mathbb{C}, \Delta_j \in \mathbb{C}^{q_j \times q_j}, \textstyle\sum_{i=1}^{\ell} q_i + \sum_{j=1}^{s} q_j = q\}, \end{aligned} \tag{4.2}$$

See [JDZ91] for details.

Let $\mathcal{K}$ be the set of all controllers that asymptotically stabilizes G. We seek a full-order strictly proper controller with realization $A_c \in \mathbb{R}^{n\times n}$, $B_c \in \mathbb{R}^{p\times n}$, $C_c \in \mathbb{R}^{m\times n}$, that is

$$K = C_c(sI - A_c)^{-1}B_c \in \mathcal{K}, \tag{4.3}$$

which solves the optimization problem

$$\inf_{K\in\mathcal{K}} \inf_{W\in\mathcal{W}_\Delta} \left\| W^{-\frac{1}{2}} \mathcal{F}_\ell(G,K) W^{\frac{1}{2}} \right\|_\infty, \tag{4.4}$$

where $\mathcal{F}_\ell(G,K) := G_{zw} + G_{zu}K\left(I - G_{yu}K\right)^{-1} G_{yw}$ is the closed-loop transfer-function from w to

z in Fig. 4.3 and

$$\mathcal{W}_\Delta = \{W : W \succ 0,\, W\Delta = \Delta W,\, \forall \Delta \in \mathcal{D}_\Delta\}. \tag{4.5}$$

The motivation behind solving problem (4.4) is that a necessary and sufficient condition (see [Sha94]) for robust stability of the interconnection in Figure 4.2 with a time-varying and norm-bounded Δ, i.e. $\|\Delta\| \leq \gamma^{-1}$, is the existence of frequency-independent multipliers W such that

$$\inf_{W \in \mathcal{W}_\Delta} \|W^{-\frac{1}{2}}\, \mathcal{F}_\ell(G,K)\, W^{\frac{1}{2}}\|_\infty < \gamma. \tag{4.6}$$

The well known small gain condition is obtained from (4.6) by the choice of $W = I$. Note also that the existence of frequency-independent multipliers is no longer necessary for robust stability if Δ is time-invariant or has bounded rates of variation (see [JDZ91, Sha94]).

Unfortunately, there exists no formulation of problem (4.4) that can lead to an efficient solution algorithm. The standard procedure is to iterate between the following two problems

$$\gamma(W) = \inf_{K \in \mathcal{K}} \left\| W^{-\frac{1}{2}}\, \mathcal{F}_\ell(G,K) W^{\frac{1}{2}} \right\|_\infty, \tag{4.7}$$

$$\eta(K) = \inf_{W \in \mathcal{W}_\Delta} \left\| W^{-\frac{1}{2}}\, \mathcal{F}_\ell(G,K) W^{\frac{1}{2}} \right\|_\infty \tag{4.8}$$

to produce a sequence of non-increasing costs. The above algorithm is known as the D-K iterations [JDZ91]. Each sub-problem can be efficiently solved with the help of semi-definite programs. For a given multiplier W, problem (4.7) is a standard H_∞ control problem, which can be solved with the following Lemma.

4.4.1 Small Gain with Multiplier: LMI version

Lemma 8 (H_∞ control with multiplier)**.** *Let $W \in \mathcal{W}_\Delta$ be given. There exists a strictly proper dynamic output feedback controller K of the form* (4.3) *that stabilizes system G given in* (4.1) *such that $\|W^{-\frac{1}{2}}\mathcal{F}_\ell(G,K)W^{\frac{1}{2}}\|_\infty < \gamma$, if and only if there exists $X \in \mathbb{S}^n$, $Y \in \mathbb{S}^n$, $Q \in \mathbb{R}^{n\times n}$, $L \in \mathbb{R}^{m\times n}$, $F \in \mathbb{R}^{n\times q}$ satisfying the following LMIs*

$$\Omega(\gamma,X,Y,Q,L,F\,|W) \prec 0, \quad \begin{bmatrix} X & I \\ I & Y \end{bmatrix} \succ 0, \tag{4.9}$$

where $\Omega(\gamma,X,Y,Q,L,F\,|W)$ is

$$\Omega(\gamma,X,Y,Q,L,F\,|W) = \begin{bmatrix} AX+XA^T+B_uL+L^TB_u^T & (\bullet)^T & (\bullet)^T & (\bullet)^T \\ Q+A^T & A^TY+YA+FC_y+C_y^TF^T & (\bullet)^T & (\bullet)^T \\ C_zX+D_{zu}L & C_z & -\gamma W & (\bullet)^T \\ B_w^T & (YB_w+FD_{yw})^T & D_{zw}^T & -\gamma W^{-1} \end{bmatrix}, \tag{4.10}$$

One such controller is given by

$$\begin{bmatrix} A_c & B_c \\ C_c & D_c \end{bmatrix} = \begin{bmatrix} V & YB_u \\ 0 & I \end{bmatrix}^{-1} \begin{bmatrix} Q-YAX & F \\ L & 0 \end{bmatrix} \begin{bmatrix} U & 0 \\ C_yX & I \end{bmatrix}^{-1} \tag{4.11}$$

in which U and V are non-singular such that $YX+VU=I$.

Proof. : The lemma is proved in [SGC97] for $W=I$. In order to obtain (4.10), set $D_c=0$ and introduce a multiplier W as in $W^{-\frac{1}{2}}\mathcal{F}_\ell(G,K)W^{\frac{1}{2}}$ and repeat the same steps as in [SGC97]. □

Unfortunately it is not possible to simultaneously optimize over the controller and the multiplier W without destroying convexity of the associated inequalities. However, the set of

matrix inequalities above is linear if W is fixed, which motivates problem (4.7). Furthermore, the existence of a multiplier $W \in \mathcal{W}_\Delta$ such that (4.6) is satisfied can be equivalently verified by establishing the existence of a feasible solution to the set of LMIs known as the scaled Bounded Real Lemma [AG95].

Lemma 9 (Scaled Bounded Real Lemma [AG95]). *Let $G = C(sI - A)^{-1}B + D$ be square and have minimal realization, and consider an uncertainty matrix $\Delta \in \mathcal{D}_\Delta$ and the associated multiplier $W \in \mathcal{W}_\Delta$ defined in* (4.2) *and* (4.5)*. The following statements are equivalent.*

i) A is Hurwitz and there exists $W \in \mathcal{W}_\Delta$ such that $\|W^{-\frac{1}{2}} G W^{\frac{1}{2}}\|_\infty < \gamma$.

ii) There exist $W \in \mathcal{W}_\Delta$ and a positive definite matrix $X \succ 0$ satisfying the following LMI

$$\begin{bmatrix} A^T X + XA & XC_z^T & B_w W \\ C_z X & -\gamma W & D_{zw} W \\ W B_w^T & W D_{zw}^T & -\gamma W \end{bmatrix} \prec 0. \tag{4.12}$$

4.5 D-K Iteration

The original D-K iteration is stated in frequency domain by first fixing an initialization D_0 across frequency and then solve the H_∞ problem to search for the optimal controller $\hat{K}$ with respect to the D_0. Then fix the controller and solve again the H_∞ problem to search for the new scaling matrix D.

The original D-K algorithm can be found in [ZD98, Section 10.4]. Here, we shall state the D-K algorithm using LMIs and the H_∞ lemma stated above.

Algorithm 1 (D-K Iterations LMI). *Choose an initial multiplier $D_0 \in W_\Delta$ and a positive $\varepsilon > 0$, set $k = 1$ and iterate:*

1. *Solve the $\mathcal{H}_\infty$ minimization problem in K*

$$\inf_{\gamma, K \in \mathcal{K}} \{\gamma : \|D_{k-1}^{-\frac{1}{2}} \mathcal{F}_\ell(G,K) D_{k-1}^{\frac{1}{2}}\|_\infty < \gamma\},$$

using Lemma 8 with a given multiplier D_{k-1} and denote (γ_k, K_k) its optimal solution.

2. *Solve the minimization problem in D*

$$\inf_{\eta, D \in \mathcal{W}_\Delta} \{\eta : \|D^{-\frac{1}{2}} \mathcal{F}_\ell(G,K_k) D^{\frac{1}{2}}\|_\infty < \eta\},$$

using the scaled Bounded Real Lemma [AG95] with a given controller K_k by performing a bisection on the cost η and denote (η_k, D_k) its optimal solution.

3. *If $\gamma_k - \eta_k < \varepsilon\gamma_0$, stop. Otherwise increment k and go to 1.*

The above algorithm produces a sequence of non-increasing cost values [ZD98]. There are no guarantees of convergence to the optimal global minimum.

Remark 13. *Because problem* (4.8) *is not an LMI, a bisection is needed to minimize η in Step 2. The key properties are: 1) that for a given η, the scaled Bounded Real Lemma [AG95] is an LMI; 2) the cost function in problem* (4.8) *is monotonic in η. This means that a solution close to the optimum can be obtained quickly (rate of 2^{-k}, where k is the number of iterations) for a given finite tolerance. Note that the tolerance of the bisection has to be chosen small enough so as not to impact other properties of the algorithm.*

4.6 An Alternative Algorithm: F-L Iteration

In this section we introduce a pair of LMIs for output-feedback robust control design using multipliers that can provide an alternative to the D-K iterations.

The main feature of this alternative formulation is the fact that the multipliers are optimized in every step of the algorithm, in contrast to the D-K iterations, in which the multiplier is held fixed whenever a controller is redesigned. The driving force behind this alternative algorithm is the following lemmas, proved in Appendices 4.9.2 and 4.9.3.

Lemma 10. *Let $\Theta \in \mathbb{R}^{m\times n}$ such that $A_\Theta = A + B_u\Theta$, $C_\Theta = C_z + D_{zu}\Theta$, with A_Θ Hurwitz be given. If there exist $S \in \mathbb{S}^n$, $Y \in \mathbb{S}^n$, $P \in \mathbb{R}^{n\times n}$, $F \in \mathbb{R}^{n\times q}$, and $\Sigma \in \mathcal{W}_\Delta$ satisfying the following LMIs*

$$\Phi(S,Y,P,F,\Sigma\,|\Theta,\gamma) \prec 0, \qquad Y \succ S, \qquad S \succ 0, \tag{4.13}$$

where

$$\Phi(S,Y,P,F,\Sigma\,|\Theta,\gamma) = \begin{bmatrix} SA_\Theta + A_\Theta^T S & (\bullet)^T & (\bullet)^T & (\bullet)^T \\ P + A^T S & YA + A^T Y + FC_y + C_y^T F^T & (\bullet)^T & (\bullet)^T \\ \Sigma C_\Theta & \Sigma C_z & -\gamma\Sigma & (\bullet)^T \\ B_w^T S & (YB_w + FD_{yw})^T & D_{zw}^T\Sigma & -\gamma\Sigma \end{bmatrix}, \tag{4.14}$$

then the controller K with realization

$$\begin{bmatrix} A_c & B_c \\ C_c & D_c \end{bmatrix} = \begin{bmatrix} S-Y & 0 \\ 0 & I \end{bmatrix}^{-1} \begin{bmatrix} P - YA_\Theta - FC_y & F \\ \Theta & 0 \end{bmatrix} \tag{4.15}$$

stabilizes system G given in (4.1) *such that $\|\Sigma^{\frac{1}{2}}\mathcal{F}_\ell(G,K)\Sigma^{-\frac{1}{2}}\|_\infty < \gamma$.*

Proof. See Appendix 4.9.2. □

Lemma 11. *Let $\Lambda \in \mathbb{R}^{n\times p}$ such that $A_\Lambda = A + \Lambda C_y$, $B_\Lambda = B_w + \Lambda D_{yw}$, with A_Λ Hurwitz be given. If there exist $Z \in \mathbb{S}^n$, $X \in \mathbb{S}^n$, $\Pi \in \mathbb{R}^{n\times n}$, $L \in \mathbb{R}^{m\times n}$, and $W \in \mathcal{W}_\Delta$ satisfying the following LMIs*

$$\Psi(Z,X,\Pi,L,W\,|\Lambda,\eta) \prec 0, \qquad X \succ Z, \qquad Z \succ 0, \tag{4.16}$$

where

$$\Psi(Z,X,\Pi,L,W\,|\Lambda,\eta)=\begin{bmatrix}(AX+B_uL)+(AX+B_uL)^T & (\bullet)^T & (\bullet)^T & (\bullet)^T\\ \Pi+ZA^T & ZA_\Lambda^T+A_\Lambda Z & (\bullet)^T & (\bullet)^T\\ (C_zX+D_{zu}L) & C_zZ & -\eta W & (\bullet)^T\\ WB_w^T & WB_\Lambda^T & WD_{zw}^T & -\eta W\end{bmatrix}, \quad (4.17)$$

then the controller K with realization

$$\begin{bmatrix}A_c & B_c\\ C_c & D_c\end{bmatrix}=\begin{bmatrix}\Pi-A_\Lambda X-B_uL & \Lambda\\ L & 0\end{bmatrix}\begin{bmatrix}Z-X & 0\\ 0 & I\end{bmatrix}^{-1} \quad (4.18)$$

stabilizes the system in (4.1) *such that* $\|W^{-\frac{1}{2}}\mathcal{F}_\ell(G,K)W^{\frac{1}{2}}\|_\infty<\eta$.

A key property of the inequalities in the above theorems is the fact that the multipliers, Σ in Lemma 10 and W in Lemma 11, can be optimized simultaneously with the controller. Note however that this has been obtained by constraining parts of the controllers to be fixed, namely the feedback gains Θ in Lemma 10 and Λ in Lemma 11.

As we will prove later in Theorem 5, one can construct a feasible solution to the inequalities in Lemma 11 from the feasible solutions to the inequalities in Lemma 10, and vice-versa. This motivates the following alternative to the D-K iterations.

Algorithm 2 (F-L Iterations)**.** *Choose an initial multiplier* $W_0\in\mathcal{W}_\Delta$ *and solve the optimization problem*

$$\inf_{\gamma,X,Y,Q,L,F}\left\{\gamma:\Omega(\gamma,X,Y,Q,L,F\,|W_0)\prec 0,\begin{bmatrix}X & I\\ I & Y\end{bmatrix}\succ 0.\right\} \quad (4.19)$$

Denote $(\gamma_0,X_0,Y_0,Q_0,L_0,F_0)$ *its optimal solution, calculate* $\Theta_0=L_0X_0^{-1}$*, select a positive* $\varepsilon>0$*, set* $k=1$*, and iterate:*

1. *Solve the optimization problem*

$$\inf_{\gamma,S,Y,P,F,\Sigma\in\mathcal{W}_\Delta} \{\gamma : \Phi(S,Y,P,F,\Sigma|\Theta_{k-1},\gamma_{k-1}) \prec 0, Y \succ S, S \succ 0\} \quad (4.20)$$

by performing a bisection on the cost γ*. Denote* $(\gamma_k, S_k, Y_k, P_k, F_k, \Sigma_k)$ *its optimal solution, calculate* $\Lambda_k = Y_k^{-1} F_k$*, and go to the next step.*

2. *Solve the optimization problem*

$$\inf_{\eta,Z,X,\Pi,W\in\mathcal{W}_\Delta} \{\eta : \Psi(Z,X,\Pi,L,W|\Lambda_k,\eta_k) \prec 0, \quad X \succ Z, Z \succ 0\} \quad (4.21)$$

by performing a bisection on the cost η*. Denote* $(\eta_k, Z_k, X_k, \Pi_k, L_k, W_k)$ *its optimal solution, calculate* $\Theta_k = L_k X_k^{-1}$*, and go to the next step.*

3. *If* $\gamma_k - \eta_k < \varepsilon\gamma_0$ *then stop. Otherwise, let* $k \leftarrow k+1$ *and go to Step 1.*

Remark 14. *Compared with the D-K iterations, each step of the F-L iteration simultaneously optimizes the complete multiplier,* Σ *in Lemma 10 and* W *in Lemma 11, and parts of the controller. As it will be illustrated in the examples, this often means that the F-L iteration converges faster than the D-K iteration, which alternates between holding the controller fixed while optimizing the multiplier and vice-versa.*

Remark 15. *From a computational complexity point of view, the steps in both algorithms are comparable. Indeed, they both iterate over LMIs with roughly the same number of variables and size of the inequalities.*

Remark 16. *As it is made clear in the proof of Lemmas 10 and 11, the LMIs in both problems are related by a congruence transformation and are independent of the final coordinates of the controller, which makes it easy to numerically transition between the two problems. In contrast, the D-K iteration requires the calculation of a controller realization, i.e. from* (Q, L, F)

to (A_c, B_c, C_c) *in* (4.11)*, every time before the multiplier is to be optimized, which can lead to numerical conditioning issues in many instances.*

The order of the Steps 1 and 2 in the F-L iterations could be swapped, that is, Step 1 could be solved after Step 2, if initialized with $\Lambda_0 = Y_0^{-1} F_0$. In the next theorem we prove that the F-L iteration produces a sequence of non-increasing cost values.

Theorem 5. *Let* γ_k *and* η_k *be the optimal costs produced at each step of Algorithm 2 in problems* (4.20)*, and* (4.21)*, respectively during the k-th iteration. Then* $\gamma_k \leq \eta_{k-1} \leq \gamma_{k-1}$*, for all* $k = 1, 2, \cdots$.

4.7 Examples

In this section we illustrate and compare the D-K and F-L iterations with two detailed examples from [Lei06]. In Section 4.8 we will present the results of a benchmark with all problems from the COMPleib library. All problems were solved on an Intel(R) Core(TM) i7-6800K CPU at 3.40GHz and 32.0GB RAM, using Mosek [mos10] with Yalmip [Lof04] in MATLAB.

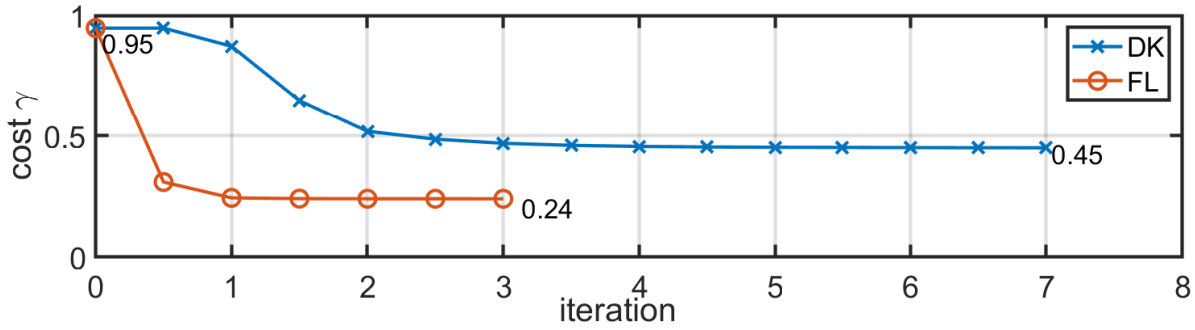

4.4(a) Example: DIS2

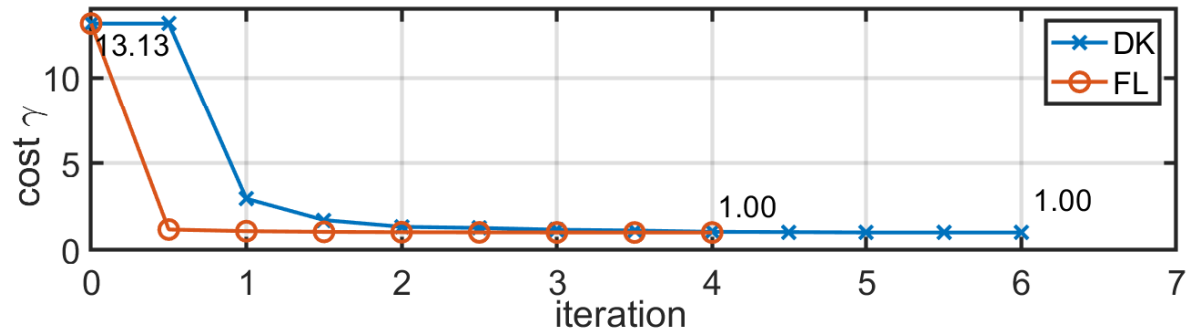

4.4(b) Example: NN1

Figure 4.4: Progression of Iterations

4.7.1 Example: DIS2

The first example is one in which the F-L iterations perform much better than the D-K iterations. The plant data ($n = 3$) is given by

$$G = \left[\begin{array}{ccc|ccc|c} 0 & 1 & 0 & 1 & 0 & 0 & 0 \\ 0 & 0 & 1 & 0 & 1 & 0 & 0 \\ 0 & 13 & 0 & 0 & 0 & 1 & 1 \\ \hline 1 & 0 & 0 & 0 & 0 & 0 & 0 \\ 0 & 1 & 0 & 0 & 0 & 0 & 0 \\ 0 & 0 & 1 & 0 & 0 & 0 & 1 \\ \hline 0 & 5 & -1 & 0 & 0 & 0 & 0 \\ -1 & -1 & 0 & 0 & 0 & 0 & 0 \end{array}\right].$$

Since this example was not originally a robust control problem, in order to fit the problem statement of the present chapter, we consider a diagonal uncertainty Δ.

We ran the D-K iterations (Algorithm 1) and the F-L iterations (Algorithm 2) both with $\varepsilon = 10^{-4}$ and starting at $D_0 = W_0 = I$. The relative tolerance for the bisections was set at $\varepsilon = 10^{-6}$. Detailed step-by-step progress of both algorithms is shown in Fig. 4.4(a). In this example, Algorithm 2 not only converges much faster, but also achieves a much lower cost. A breakdown of the cost and the total number of iterations and LMIs solved is given as the first row of Table 4.1, showing the initial cost γ_0, the final cost γ_k, the improvement of both algorithms relative to the initial cost, $\rho = 1 - \gamma_k/\gamma_0$, and the improvement of the F-L iterations relative to the D-K iterations, $\mu = (\gamma_k^{\mathrm{DK}} - \gamma_k^{\mathrm{FL}})/\gamma_0$, as well as the total number of LMIs solved by each algorithm and the total time is seconds. In this example, the total time as well as the number of LMIs solved is similar, even though the number of iterations taken by each algorithm is different. The F-L iterations produce a final cost that is 22% less than the one produced by the D-K iterations

when compared with the initial cost. In absolute terms, the F-L cost is 53% smaller than the D-K iterations.

4.7.2 Example: NN1

The second example is one in which the F-L iterations and the D-K iterations perform similarly. Data for this example ($n = 3$) is given by

$$G = \left[\begin{array}{ccc|ccc|cc} -4 & 2 & 1 & 1 & 0 & 0 & 1 & 0 \\ 3 & -2 & 5 & 0 & 1 & 0 & 1 & 0 \\ -7 & 0 & 3 & 0 & 0 & 1 & 0 & 1 \\ \hline 1 & 0 & 0 & 0 & 0 & 0 & 0 & 0 \\ 0 & 1 & 0 & 0 & 0 & 0 & 1 & 0 \\ 0 & 0 & 1 & 0 & 0 & 0 & 0 & 1 \\ \hline 0 & 1 & 0 & 0 & 0 & 0 & 0 & 0 \\ 0 & 0 & 1 & 0 & 0 & 0 & 0 & 0 \end{array}\right].$$

Detailed step-by-step progress of both algorithms are shown in Fig. 4.4(b). In this example, both algorithm converge to a similar final cost, with the F-L iterations again converging faster.

4.8 Benchmark and Conclusions

In order to compare the performance of the D-K and F-L iterations we attempted[1,2] to run all 81 problems from [Lei06] with the same settings used in Examples 4.7.1 and 7. We successfully solved a total of 50 examples, with the results summarized in Table 4.1. The F-L

[1]Yalmip and Mosek failed to solve the initialization problem (4.19) for the following problems: AC7, AC10, AC12, AC13, AC14, AC18, JE1, JE2, REA3, REA4, TG1, WEC1, WEC2, WEC3, BDT2, UWV, CSE2, PAS, TF2, NN3, NN5, NN6, NN7, NN11, NN17.

[2]The following problem were too large to fit into our computer memory: HF1($n = 130$), BDT2($n = 82$), EB6($n = 160$), TL($n = 256$), CDP($n = 120$), NN18($n = 1006$).

iterations improved the minimum cost by more than 1% in 26 out of the 50 problems solved, and by more than 15% in 13 out of 50 problems. The largest improvement obtained was about 58% in problem HE6. In 23 out of 50 problems, the final cost was about the same as with the D-K iterations. The results are summarized in Tab. 4.2.

In the same table we also attempt to summarize the time it took to solve the same problems using the F-L versus the D-K iterations. Due to the large variation in problem dimensions and data conditioning, directly comparing the computational time does not seem to lead to strong conclusions. However, as shown in Table 4.2, it is possible to conclude that the cost improvements obtained by the F-L iterations will come associated with longer computational times. One is refered to the complete time results in Table 4.1 for time results on specific instances.

In only 1 problem out of 50 the D-K iterations performed better than the F-L iterations (DIS3). In this case, the F-L iterations stopped earlier than the D-K iterations. However, it should be noted that if the tolerance ε is reduced, then the F-L iterations will also converge to a cost that is similar to the one attained by the D-K iterations.

In conclusion, the proposed F-L iterations seem to be a viable alternative to the classic D-K iterations, often providing improved cost. After tuning the tolerances in the algorithms we could not find any instance in the COMPleib set of problems in which the D-K algorithm produced a significantly better cost. The run times and number of LMIs solved by each algorithm are similar.

4.9 Proofs

4.9.1 Proof to Theorem 5

Proof. We first prove that $\gamma_1 \leq \gamma_0$. If the solution to problem (4.19) is $(\gamma_0, X_0, Y_0, Q_0, L_0, F_0)$, then we have $\Omega(\gamma_0, X_0, Y_0, Q_0, L_0, F_0 \,|W_0) \prec 0$. Because $X_0 \succ 0$ and $W_0 \in \mathcal{W}_\Delta'$, then the congruence

matrix $T = \mathrm{diag}(X_0^{-1}, I, W_0^{-1}, I)$ is non-singular and

$$T^T \, \Omega(\gamma_0, X_0, Y_0, Q_0, L_0, F_0 \,|W_0)\, T \prec 0.$$

The choice of variables

$$S = X_0^{-1}, \qquad Y = Y_0, \qquad P = Q_0 X_0^{-1}, \qquad F = F_0, \qquad \Sigma = W_0^{-1}$$

is such that $\Sigma \in \mathcal{W}_\Delta$, $Y = Y_0 \succ X_0^{-1} = S \succ 0$, and, as one can verify that with $\Theta_0 = L_0 X_0^{-1}$,

$$\Phi(S, Y, P, F, \Sigma \,|\Theta_0, \gamma_0) = T^T \, \Omega(\gamma_0, X_0, Y_0, Q_0, L_0, F_0 \,|W_0)\, T \prec 0,$$

which implies that $(\gamma_0, S, Y, P, F, \Sigma)$ is a feasible solution to the optimization problem (4.20) in Step 1, that is that $\gamma_1 \leq \gamma_0$.

Next we prove that $\eta_k \leq \gamma_k$, $k \geq 1$. If the solution to problem (4.20) in Step 1 is $(\gamma_k, S_k, Y_k, P_k, F_k, \Sigma_k)$ then

$$\Phi(S_k, Y_k, P_k, F_k, \Sigma_k \,|\Theta_{k-1}, \gamma_k) \prec 0.$$

Because $S_k \succ 0$, $Y_k \succ 0$, the choice of variables

$$\eta = \gamma_k, \qquad Z = Y_k^{-1}, \qquad X = S_k^{-1},$$
$$\Pi = Y_k^{-1} P_k S_k^{-1}, \qquad L = \Theta_k S_k^{-1}, \qquad W = \Sigma_k^{-1}$$

is such that $W \in \mathcal{W}_\Delta$, $T = \mathrm{diag}(S_k^{-1}, Y_k^{-1}, \Sigma_k^{-1}, \Sigma_k^{-1})$ is non-singular, $X = S_k^{-1} \succ Y_k^{-1} = Z \succ 0$,

and

$$\Psi(Z,X,\Pi,L,W\,|\Lambda_k,\eta) = T^T\,\Phi(S_k,Y_k,P_k,F_k,\Sigma_k\,|\Theta_{k-1},\gamma_k)\,T \prec 0.$$

with $\Lambda_k = Y_K^{-1}F_k$, which implies that (η,Z,X,Π,L,W) is a feasible solution to the optimization problem (4.21) in Step 2, that is that $\eta_k \leq \eta = \gamma_k$.

Finally, denote by $(\eta_{k-1},Z_{k-1},X_{k-1},\Pi_{k-1},L_{k-1},W_{k-1})$ the solution to problem (4.21) in Step 2 such that

$$\Psi(Z_{k-1},X_{k-1},\Pi_{k-1},L_{k-1},W_{k-1}\,|\Lambda_{k-1},\eta_{k-1}) \prec 0.$$

Because $Z_{k-1} \succ 0$, $X_{k-1} \succ 0$, the choice of variables

$$\begin{aligned} &\gamma = \eta_{k-1}, && S = X_{k-1}^{-1}, && Y = Z_{k-1}^{-1}, \\ &P = Z_{k-1}^{-1}\Pi_{k-1}X_{k-1}^{-1}, && F = Z_{k-1}^{-1}\Lambda_{k-1}, && \Sigma = W_{k-1}^{-1}, \end{aligned}$$

is such that $T = \mathrm{diag}(X_{k-1}^{-1},Z_{k-1}^{-1},W_{k-1}^{-1},W_{k-1}^{-1})$ is non-singular with $Y = Z_{k-1}^{-1} \succ X_{k-1}^{-1} = S \succ 0$ and $\Sigma \in \mathcal{W}_\Delta$. One can verify that, with $\Theta_{k-1} = L_{k-1}X_{k-1}^{-1}$,

$$\Phi(S,Y,P,F,\Sigma\,|\Theta_{k-1},\gamma) = T^T\Psi(Z_{k-1},X_{k-1},\Pi_{k-1},L_{k-1},W_{k-1}\,|\Lambda_{k-1},\eta_{k-1})\;T \prec 0,$$

implying that (γ,S,Y,P,F,Σ) is a feasible solution to the optimization problem (4.20) in Step 1, i.e. $\gamma_k \leq \gamma = \eta_{k-1}$. □

4.9.2 Proof of Lemma 10

Let (S,Y,P,F,Σ) be such that (4.13) is satisfied and $\Sigma \in \mathcal{W}_\Delta'$. Then $S \succ 0$ and the choice of variables

$$X = S^{-1}, \qquad Q = PS^{-1}, \qquad L = \Theta S^{-1}, \qquad W = \Sigma^{-1},$$

is such that $Y \succ X^{-1}$, that is $T = \mathrm{diag}(S^{-1}, I, \Sigma^{-1}, I)$ is non-singular so that

$$\Omega(\gamma, X, Y, Q, F, L\,|W) = T^T \Phi(S, Y, P, F, \Sigma\,|\Theta, \gamma)\, T \prec 0.$$

This means that (γ, X, Y, Q, F, L) satisfy the inequalities in Lemma8. Controller (4.15) is (4.11) after the choice of

$$U = S^{-1} = X \succ 0, \qquad V = S - Y = X^{-1} - Y \succ 0,$$

and $A_\Theta = A + B_u\Theta$.

4.9.3 Proof of Lemma 11

A proof is similar to the proof of Lemma 10 starting from (4.16) with the choice of variables

$$\eta = \gamma, \qquad Y = Z^{-1}, \qquad Q = Z^{-1}\Pi, \qquad F = Z^{-1}\Lambda,$$

such that $X \succ Y^{-1}$, $T = \mathrm{diag}(I, Z^{-1}, I, W^{-1})$ non-singular implies

$$\Omega(\gamma, X, Y, Q, F, L\,|W) = T^T \Psi(Z, X, \Pi, L, W\,|\Lambda, \eta)\, T \prec 0,$$

and the choice of controller (4.18) follows from $A_\Lambda = A + \Lambda C_y$,

$$U = Z - X = Y^{-1} - X \succ 0, \qquad\qquad V = Z^{-1} = Y \succ 0,$$

and (4.11).

4.10 Acknowledgment

Chapter 4, in full, is a reprint of the material as it appears in: Chen, Yilong, and Mauricio C. de Oliveira. "An Alternative Algorithm to the DK Iterations for Robust Control Design." IEEE Control Systems Letters 5.1 (2020): 115-120. The dissertation author was the primary investigator and author of this material.

Table 4.1: Results of feasible *COMPl$_e$ib* examples. The columns status denotes criterion used to interrupt the algorithms: CV (Converged), LP (Lack of Progress), NP (Numerical Problems).

			D-K						F-L						
Name	n	γ_0	γ_k	ρ (%)	k	# LMIs	t	Status	γ_k	ρ (%)	μ (%)	k	# LMIs	t	Status
NN2	2	1.8E+00	1.8E+00	0.0	2	42	5.9	CV	1.8E+00	0.7	0.7	2	61	8.9	LP
DIS2	3	9.5E-01	4.5E-01	52.4	13	273	41.5	CV	2.4E-01	74.6	22.2	6	241	36.9	CV
NN1	3	1.3E+01	1.0E+00	92.4	11	231	34.6	LP	1.0E+00	92.4	-0.0	8	321	51.3	LP
NN8	3	2.4E+00	2.1E+00	12.5	7	147	23.0	CV	2.1E+00	12.6	0.0	8	301	48.6	CV
NN15	3	9.8E-02	1.0E-05	100.0	5	105	17.5	NP	2.0E-04	99.8	-0.2	6	221	36.9	CV
AC4	4	5.6E-01	4.1E-02	92.6	6	168	25.1	LP	2.1E-02	96.2	3.6	3	136	22.4	LP
AC5	4	7.0E+02	1.2E+02	82.8	4	112	16.1	NP	1.2E+02	83.4	0.5	4	217	33.2	LP
AC15	4	1.5E+01	7.3E-02	99.5	9	252	41.0	NP	9.1E-02	99.4	-0.1	5	271	43.2	LP
AC16	4	1.5E+01	1.0E-02	99.9	6	168	28.4	LP	1.7E-02	99.9	-0.0	8	406	67.3	LP
AC17	4	6.6E+00	1.7E+00	73.9	5	140	20.5	CV	1.7E+00	74.1	0.2	3	163	25.0	LP
HE1	4	7.4E-02	7.4E-02	0.0	1	28	3.5	CV	7.3E-02	1.2	1.2	5	271	43.1	CV
HE2	4	2.4E+00	1.8E+00	27.4	4	112	16.3	LP	1.6E+00	35.4	8.0	5	271	44.1	CV
REA1	4	8.6E-01	2.9E-01	66.7	21	441	65.0	LP	2.7E-01	68.6	1.9	5	181	27.7	CV
REA2	4	1.1E+00	6.4E-01	43.3	20	400	59.8	LP	6.3E-01	44.2	1.0	4	141	23.4	LP
DIS5	4	6.7E+02	6.3E+02	5.3	4	84	13.3	NP	4.0E+02	40.5	35.2	3	121	20.2	LP
MFP	4	4.2E+00	2.5E+00	41.1	10	210	33.0	LP	1.7E+00	60.0	18.9	3	121	20.4	LP
NN4	4	1.3E+00	8.3E-01	35.7	19	399	63.0	LP	8.1E-01	37.3	1.5	9	361	57.9	LP
AC2	5	1.1E-01	2.8E-02	75.1	18	504	88.4	LP	2.8E-02	75.1	0.0	6	298	50.0	LP
AC3	5	3.0E+00	2.3E+00	22.9	8	224	35.6	LP	2.3E+00	22.9	0.1	7	379	65.1	LP
AC11	5	2.8E+00	7.6E-02	97.3	8	197	35.4	CV	5.0E-02	98.2	0.9	7	352	62.2	LP
NN9	5	1.4E+01	1.3E+01	2.8	2	22	4.0	NP	9.1E+00	33.5	30.8	6	241	46.1	LP
DIS3	6	1.0E+00	2.6E-01	74.7	25	525	103.3	LP	6.8E-01	35.2	-39.4	4	141	27.2	LP
DIS4	6	7.3E-01	4.9E-01	33.2	81	1701	320.1	CV	4.5E-01	39.0	5.8	2	61	11.5	CV
NN12	6	6.3E+00	5.8E+00	8.4	2	42	7.3	CV	3.9E+00	38.2	29.7	4	141	26.9	LP
NN13	6	1.0E+01	1.0E+01	0.0	1	21	3.5	CV	9.2E+00	9.3	9.3	3	121	22.5	LP
NN14	6	9.4E+00	9.0E+00	4.4	3	63	11.4	CV	8.4E+00	11.1	6.6	3	121	22.0	LP
AC6	7	3.4E+00	5.2E-01	84.7	8	197	38.3	NP	3.6E-01	89.5	4.8	6	325	65.5	CV
TF1	7	2.5E-01	5.2E-02	78.9	8	168	34.2	CV	2.3E-02	90.8	11.9	4	161	31.3	LP
TF3	7	2.5E-01	1.6E-01	34.2	3	63	10.9	LP	2.4E-02	90.4	56.2	4	161	31.1	CV
PSM	7	9.2E-01	7.5E-05	100.0	4	84	17.1	CV	5.4E-04	99.9	-0.1	4	141	27.6	LP
HE3	8	8.0E-01	5.2E-04	99.9	12	336	69.8	LP	2.5E-04	100.0	0.0	3	136	29.9	LP
HE4	8	2.3E+01	1.9E+00	91.5	6	141	33.2	CV	1.4E+00	93.9	2.4	3	163	43.0	LP
HE5	8	1.8E+00	3.8E-01	78.8	21	588	133.2	CV	3.9E-01	78.0	-0.8	3	163	30.4	LP
DIS1	8	4.2E+00	2.3E-03	99.9	4	84	18.3	CV	1.9E-03	100.0	0.0	7	261	53.2	LP
NN10	8	5.2E-06	1.8E-09	100.0	3	63	14.4	CV	4.3E-11	100.0	0.0	2	61	12.7	LP
NN16	8	9.6E-01	4.5E-01	52.4	19	399	90.7	CV	4.4E-01	53.9	1.4	2	61	12.8	LP
AC8	9	1.6E+00	3.0E-01	81.7	3	84	21.1	LP	9.4E-02	94.2	12.5	2	82	26.7	LP
AC9	10	1.0E+00	7.3E-03	99.3	2	29	11.0	LP	6.5E-03	99.4	0.1	2	109	33.8	LP
EB1	10	3.1E+00	2.8E+00	10.7	15	315	73.8	LP	2.8E+00	10.8	0.0	2	81	18.5	LP
EB2	10	1.8E+00	1.8E+00	0.0	1	21	5.8	CV	1.4E+00	23.0	23.0	3	101	22.5	CV
EB3	10	1.8E+00	1.8E+00	0.0	1	21	5.5	LP	1.4E+00	23.1	23.1	3	121	25.8	LP
BDT1	11	2.7E-01	1.5E-05	100.0	7	147	46.6	CV	4.8E-04	99.8	-0.2	3	101	28.6	CV
AGS	12	8.2E+00	6.5E+00	20.7	15	295	105.6	CV	6.5E+00	21.0	0.3	5	201	69.2	LP
HE6	20	2.4E+00	2.3E+00	4.5	2	56	90.3	NP	9.0E-01	62.4	57.9	4	217	212.9	LP
HE7	20	2.6E+00	1.9E+00	27.3	3	63	106.9	LP	9.3E-01	64.5	37.2	11	441	582.8	LP
CSE1	20	2.0E-02	2.1E-05	99.9	5	105	152.4	LP	1.7E-04	99.1	-0.7	2	61	62.4	LP
EB4	20	1.8E+00	1.8E+00	0.0	1	21	25.4	LP	1.4E+00	23.1	23.1	3	101	78.0	LP
IH	21	2.8E-03	2.1E-04	92.5	2	42	109.6	LP	2.3E-04	91.9	-0.6	3	101	151.9	LP
JE3	24	2.9E+00	2.0E+00	30.0	2	42	99.5	CV	1.1E+00	63.0	33.0	2	81	171.4	LP
EB5	40	1.8E+00	1.8E+00	0.0	1	21	487.3	LP	1.4E+00	23.1	23.1	3	101	1346.6	LP

Table 4.2: Total number of feasible problems in the COMPleib library and corresponding range of percent improvement (μ) obtained by the F-L iterations as compared with the D-K iterations.

	# problems		
Cost Improvement	more time	less time	**total:**
$\mu < -1$	0	1	1
$\lvert\mu\rvert \leq 1$	14	9	23
$1 < \mu \leq 15$	7	6	13
$\mu > 15$	11	2	13
total:	32	18	50

Chapter 5

Multipliers for Phase-Locked Loop Design

Phase-locked loops (PLL) are perhaps the mostly widely deployed type of closed-loop system, being a central component in modulators and demodulators, clock generators and dividers, which are integral to modern cell phones, computers, network equipment, etc. Unsurprisingly, the analysis and design of PLLs have been extensively discussed in the literature, spanning more than a half century of research [RV76, Gup75, Abr89, Abr02b, TSS01]. More recent discussions can be found in [GMFG13, Ban16, GMF12, GGV18, KKEM18, ACH+18].

A typical PLL is comprised of the blocks shown in Fig. 5.1, in which the *Phase Detector* (PD) produces an output which is proportional to the phase difference between the *input signal*, and the signal generated locally by the *Voltage-Controlled Oscillator* (VCO), whose input is the output of the *Loop Filter* (LF). See, for example, reference [Gar05] for details. By varying which

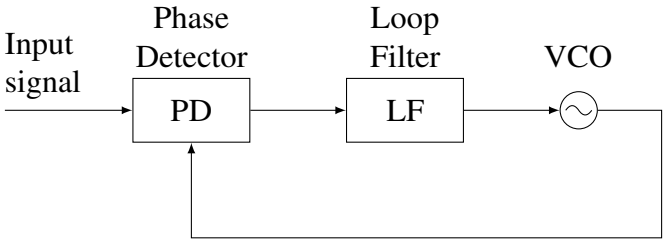

Figure 5.1: Phase-Locked Loop block-diagram (see [Gar05] for details)

signal in the loop one considers as output, this basic architecture can be used for demodulating signals, synchronizing oscillators, dividing clocks, etc. There are several variations on the type of PD and VCO, depending on the nature (digital versus analog) and application of the PLL circuit. No matter the setup, most of the features of the PLL derive from a properly designed LF. In the present chapter we focus on analog PLLs and conditions on the LF so that the closed-loop is asymptotically stable.

One difficulty faced during the design and implementation of PLLs is the unavoidable nonlinear nature of the phase detector and its interaction with the closed-loop. The presence of such nonlinearity in the loop can bring instability and performance issues that have been analyzed in the literature using a variety of techniques. In the present chapter we revisit the conditions from [Abr02b, Abr89, Eva98], which, directly or indirectly, use the Circle or the Popov Criterion [KG02b] to ensure stability of the nonlinear closed-loop. Of all these conditions, the one from [Eva98] seems to be the most general.

In this chapter, we will present the following features.

a) An alternative formulation of the stability conditions of [Eva98] in terms of the linearized closed-loop transfer-functions in Fig. 5.1 that allows for a more direct and intuitive design;

b) Unlike [Eva98], the proposed reformulation comes with a graphical test in which it is possible to directly assess and graphically optimize the maximum possible guaranteed locking range;

c) The identification of a fundamental limitation on the maximum possible guaranteed locking range for PLLs of type higher or equal than 3.

d) Various analytic and numerical results available in the literature are shown to be obtainable using the new stability criterion.

Section 5.1 provides the mathematical model used to analyse the stability of PLLs. Section 5.2 revisits the PLL stability analysis technique of [Eva98] and discusses some of their

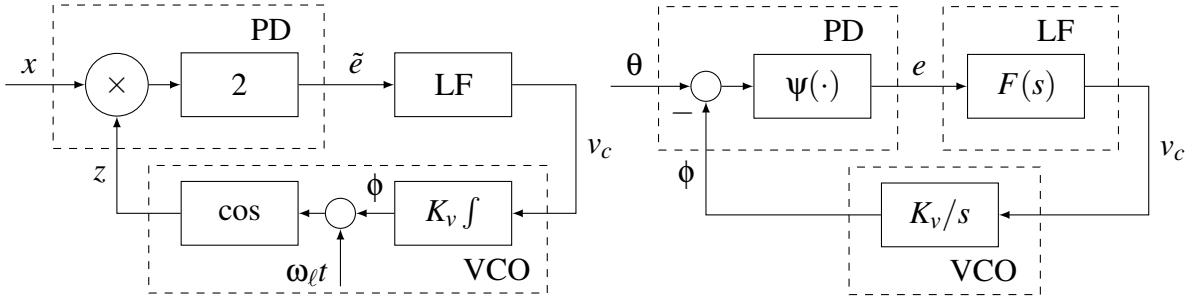

5.2(a) Multiplier Phase-Detector

5.2(b) Phase signals

Figure 5.2: Diagrams for PLL analysis and design

limitation. In Section 5.3, a new formulation of the conditions from [Eva98] is presented in a way that enables a graphical interpretation in terms of the loop transfer-function along with examples that illustrate usage of the new theorems. In Section 5.6, simulation results of various PLL system, from type-I to -III, are provided.

5.1 PLL Model

From the basic diagram in Fig.5.1 one proceeds by choosing a particular PD and VCO modules. One typical setup is the one shown in Fig. 5.2. For example, if the diagram in Fig. 5.25.2(a) is used as a coherent receiver, then

$$x(t) = \sin(\omega_c t + \theta(t)) \tag{5.1}$$

is a signal centered around the carrier frequency ω_c produced by a transmitter that is phase- or frequency-modulated by $\theta(t)$, and

$$z(t) = \cos(\omega_\ell t + \phi(t)), \qquad \phi(t) = K_v \int_0^t v_c(\tau)\, d\tau \tag{5.2}$$

is a signal produced by the receiver VCO. In Fig. 5.25.2(a), the PD is the simple multiplier circuit, which is widely used in analog PLLs, that produces as output

$$\tilde{e}(t) = 2x(t)z(t). \tag{5.3}$$

If x and z are as in (5.1) and (5.2) then

$$\tilde{e}(t) = \sin\left((\omega_c + \omega_\ell)t + \theta(t) + \phi(t)\right) + \sin\left((\omega_c - \omega_\ell)t + \theta(t) - \phi(t)\right). \tag{5.4}$$

Because the carrier frequency ω_c is often much larger than the bandwidth of the modulating signal $\theta(t)$, a low-pass filter can be safely introduced after the multiplier circuit to produce an error signal that contains just the second term above. Furthermore, it is reasonable to assume that $\omega_c \approx \omega_\ell$, either because they are both known frequencies or because the PLL will be designed so as to achieve such matching of the input and local frequencies (more on that later). This means that

$$\tilde{e}(t) \approx e(t) = \psi\left(\theta(t) - \phi(t)\right), \qquad \psi(\cdot) = \sin(\cdot).$$

The resulting phase signals are depicted in the simplified PLL diagram shown in Fig. 5.25.2(b). It is this diagram which will be used as a starting point for stability analysis of the PLL [Gar05]. See [LKYY15, KKL+15] for potential caveat using the simplified phase model.

In Fig. 5.25.2(b), the signal $e(t)$ represents the baseband component of the error signal produced by the PD, $F(s)$ is the transfer-function of a linear loop filter, and the integrator model for the VCO stems from the fact that the deviation of the VCO output signal from its center frequency is proportional to the VCO gain factor K_v, as in (5.2). Since frequency is the time-derivative of phase, the VCO can be described as $\dot{\phi}(t) = K_v v_c(t)$.

A PLL is said to be *locked* when $\omega_c = \omega_\ell$ and $e(t) = \psi(\theta(t) - \phi(t)) = 0$. Note that a

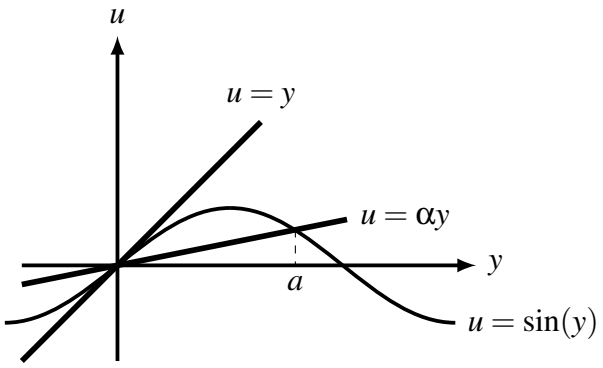

Figure 5.3: Sector Bounded $sin(\cdot)$

locked PLL will have $\theta(t) = \phi(t) + k\pi$, $k \in \mathbb{Z}$, because of the presence of the nonlinearity. In order to calculate the frequency range in which the PLL is locked, in other words, the *locking range* of PLL, we need to introduce the concept of *sector-nonlinearities* as follows.

Many forms of nonlinearities commonly used in PLLs can be accommodated by the above setup. In the present chapter, for $y \in [-a, a]$, the nonlinearity $\psi(y) = \sin(y) \in [\alpha, 1]$ where $0 < \alpha < 1$. Note that

$$a = \text{sinc}^{-1}(\alpha) \in (-\pi, \pi), \qquad \text{sinc}(x) = \frac{\sin x}{x},$$

represents the locking range of PLL, as shown in Fig. 5.3, and that the sector slope α and the locking range a are not independent. In particular, the smaller the α, the wider the locking range a.

5.2 Stability Analysis Methods

For the purpose of stability analysis, set $\theta = 0$ in Fig. 5.2 and combine the transfer functions of the individual linear elements to obtain the overall loop transfer function G and a

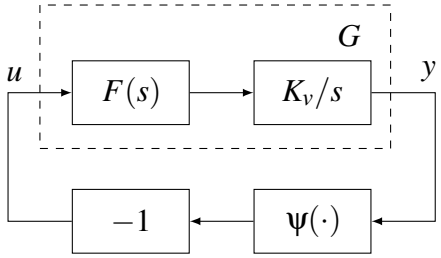

Figure 5.4: Feedback model for PLL stability analysis

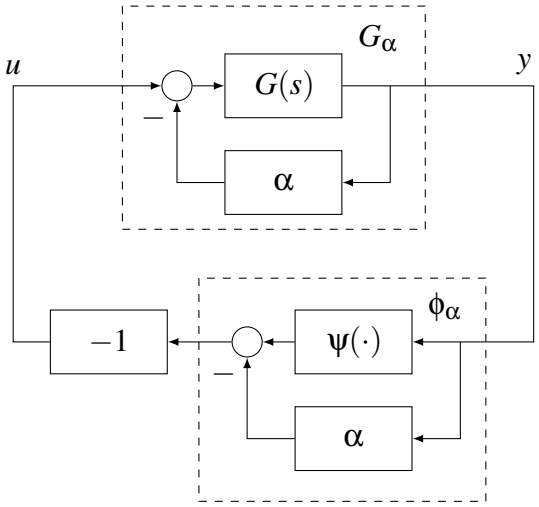

Figure 5.5: Loop Transformation from $[\alpha, 1]$ to $[0, 1-\alpha]$

nonlinearity ψ as in

$$G(s) = K_v \frac{F(s)}{s}, \qquad u = -\psi(y) = -\sin(y), \qquad \psi \in [\alpha, 1], \quad \alpha \in (0, 1], \tag{5.5}$$

so that the phase-locked loop can be represented as the feedback connection of the open-loop transfer function G and the nonlinearity ψ as shown in Fig. 5.4.

A well known sufficient condition for stability of the feedback connection of a linear system G with a sector-bounded nonlinearity as shown in Fig. 5.4 when $\psi \in [0, \infty)$, is that G be strictly positive-real [KG02b, p.265]. For a general sector $[\alpha, \beta]$, one can use a loop-transformation to shift the sector boundaries and obtain various results, such as the Circle and the Popov Criteria, as in Lemma 3.

The sector in the above criterion is $\psi \in [0,k],\ k > 0$. In order to apply this result to the stability analysis of PLLs, various authors have performed a loop-transformation, shown in Figure 5.5, to the system and sector in (5.5) to arrive at the equivalent system and sector

$$G_\alpha(s) = \frac{G(s)}{1+\alpha G(s)}, \qquad \phi_\alpha(y) = \psi(y) - \alpha y, \qquad \phi_\alpha \in [0, 1-\alpha], \tag{5.6}$$

which is in a form suitable to Lemma 3.

In fact, many papers in the literature have implicitly or explicitly used the Circle Criterion [Eva98] as well as the Popov Criterion [Wu02a, Abr89] to analyze the stability of PLLs. For example, the work [Eva98] transforms the original system into (5.6) to derive the following PLL stability criterion.

Lemma 12 (PLL Stability [Eva98])**.** *Consider the linear time-invariant system G in feedback with the static nonlinear function* $\psi \in [\alpha, 1],\ \alpha \in (0,1]$. *The feedback connection of G and* ψ *is absolutely stable for* $y \in [-a,a]$, $a = \mathrm{sinc}^{-1}(\alpha)$, *if* G_α, *from* (5.6)*, is asymptotically stable and there exists* $\gamma \geq 0$ *with* $(1+p_k\gamma) \neq 0$ *for every pole* p_k *of* G_α *such that*

$$1 + (1+\gamma s)(1-\alpha)G_\alpha(s) \tag{5.7}$$

is SPR.

Lemma 12 is a straightforward application of Lemma 3 to the system obtained after the loop-transformation (5.6). Note that (5.7) is simply scaled by $k = 1-\alpha > 0$. In the case of PLL stability, the introduction of G_α serves two purposes: a) bring the sector (5.5) into the form required by the Popov Criterion (5.6); b) asymptotically stabilize the open-loop PLL which is always necessary because the transfer-function G has at least one imaginary pole.

One major drawback of working with G_α instead of directly with G is that one loses the ability to perform the test in Lemma 12 graphically. Furthermore, the dependence on G_α on

the sector parameter α, means that the search for α and γ has to be iterative, since analytic or graphical methods for evaluating the positive realness of (5.7) will require a given G_α. Indeed, one of the goals of this chapter in revisiting such stability conditions is in clarifying the role played by imaginary poles and providing graphical versions of the Circle and the Popov criterion for PLL stability analysis in which the α and γ can be easily visualized and manipulated.

5.3 PLL Design

With the above discussion in mind, a different version of the Popov criterion that is better suited for the analysis of stability of PLLs is provided next.

Theorem 6. *Consider the linear time-invariant system G in feedback with the static nonlinear function* $\psi \in [\alpha, 1],\ \alpha \in (0,1]$. *The feedback connection of G and* ψ *is absolutely stable for* $y \in [-a,a]$, $a = \text{sinc}^{-1}(\alpha)$, *if H is asymptotically stable, where*

$$H(s) = \frac{G(s)}{1+G(s)}, \tag{5.8}$$

and there exists $\gamma \geq 0$ *with* $(1+p_k\gamma) \neq 0$ *for every pole* p_k *of H such that*

$$1-(1-\gamma s)(1-\alpha)H(s) \tag{5.9}$$

is SPR.

Proof. We shall use Lemma 12 to prove absolute stability. The case $\alpha = 1$ is trivial hence it is assumed that $\alpha \neq 1$. Assume also that H is asymptotically stable and that (5.9) is SPR so that

$$\frac{1}{1-\alpha} - \text{Re}\{H(j\omega)\} - \gamma\omega\,\text{Im}\{H(j\omega)\} > 0 \tag{5.10}$$

First, (5.6) and (5.8) imply that

$$G_\alpha(s) = \frac{G(s)}{1+\alpha G(s)} = \frac{\frac{G(s)}{1+G(s)}}{\frac{1}{1+G(s)} + \alpha\frac{G(s)}{1+G(s)}} = \frac{H(s)}{1-(1-\alpha)H(s)}.$$

Define ω_k, $k = 1,\dots,m$ where $\mathrm{Im}\{H(j\omega_k)\} = 0$. It can be seen that

$$\mathrm{Re}\{H(j\omega_k)\} < \frac{1}{1-\alpha}, \qquad \forall\, k = 1,\dots,m,$$

which means that the Nyquist plot of $H(j\omega)$ only intersects the real axis to the left of point $1/(1-\alpha)$. Because $H(s)$ is asymptotically stable, it does not have any purely imaginary poles, therefore the Nyquist plot never encircles $1/(1-\alpha)$. By the Nyquist stability criterion [DO17], G_α is thus also asymptotically stable.

Define

$$X(s) = (1-\alpha)\,\mathrm{Re}\{H(s)\}, \qquad Y(s) = (1-\alpha)\,\mathrm{Im}\{H(s)\},$$

such that (5.10) can be written as

$$1 - X(j\omega) - \gamma\omega Y(j\omega) > 0. \tag{5.11}$$

Note that

$$(1-X(j\omega))^2 + Y(j\omega)^2 > 0 \tag{5.12}$$

for all $\omega > 0$ because $X(j\omega) < 1$ when $Y(j\omega) = 0$. Divide (5.11) by (5.12) to arrive at

$$\mathrm{Re}\{Z(j\omega)\} = \frac{1 - X(j\omega) - \gamma\omega Y(j\omega)}{(1-X(j\omega))^2 + Y(j\omega)^2} > 0$$

in which

$$Z(s) = \frac{(1+\gamma s)(1-X(s)+jY(s))}{(1-X(s)-jY(s))(1-X(s)+jY(s))} - \gamma s.$$

One can then show that

$$\begin{aligned}
Z(s) &= \frac{1+\gamma s}{1-X(s)-jY(s)} - \gamma s \\
&= \frac{1+\gamma s(X(s)+jY(s))}{1-X(s)-jY(s)} \\
&= \frac{1-X(s)-jY(s)+(1+\gamma s)(X(s)+jY(s))}{1-X(s)-jY(s)} \\
&= 1+(1+\gamma s)\frac{X(s)+jY(s)}{1-X(s)-jY(s)} \\
&= 1+(1+\gamma s)\frac{(1-\alpha)H(s)}{1-(1-\alpha)H(s)} \\
&= 1+(1+\gamma s)(1-\alpha)G_\alpha(s)
\end{aligned}$$

which, assuming that $-1/\gamma$ is not a pole of G_α, implies that (5.7) is SPR, hence that Lemma 12 holds so that the feedback connection between G and ψ is absolutely stable for $y \in [-a,a]$, $a = \text{sinc}^{-1}(\alpha)$. Note that if $-1/\gamma$ is a pole of G_α, the above argument still holds after applying a small perturbation to γ.

□

Remark 17. *It is worth pointing out that H given by* (5.8) *is the transfer function of the unit negative feedback connection of G. Hence it must be Hurwitz because it lies in the given sector. H is also the linearized closed-loop transfer-function, which by the Lyapunov theorem [KG02b, Chapter 4, Theorem 4.7], ensures local asymptotic stability of the original nonlinear system.*

Remark 18. *Because Theorem 6 is a variant of the Popov criterion, it admits a time-domain interpretation via a carefully constructed Lyapunov function (see [KG02b, Chapter7, Theorem 7.3]). Using such a Lyapunov function one can determine a region of attraction using standard*

techniques also discussed in [KG02b].

Remark 19. *Compared with Lemma 12, one advantage of Theorem 6 is that H is independent of α and α enters* (5.9) *as a constant offset. This eliminates the necessity for an iterative search as needed for Lemma 12.*

Remark 20. *The Circle criterion can be recovered by setting $\gamma = 0$ in Theorem 6, resulting in the condition that*

$$\mathrm{Re}\{H(j\omega)\} < \frac{1}{1-\alpha},$$

in other words that $H(j\omega)$ must lie to the left of the vertical line defined by $1/(1-\alpha)$.

Remark 21. *One can obtain a variant of the Popov plot by plotting $\mathrm{Re}\{H(j\omega)\}$ versus $\omega\,\mathrm{Im}\{H(j\omega)\}$. The feedback connection is absolutely stable if $(\mathrm{Re}\{H(j\omega)\}, \omega\,\mathrm{Im}\{H(j\omega)\})$ lies to the left of the stability line which intercepts the horizontal axis at $(1-\alpha)^{-1}$ with a slope of $-1/\gamma$.*

Remark 22. *The parameter α has to be strictly positive and one can analyze the maximum locking behavior of* (5.9) *by simply setting $\alpha = 0$. If $\alpha = 0$ then G_α is not asymptotically stable because of the presence of at least on integrator in the loop. Indeed, Lemma 12 cannot be used for stability analysis if G_α is not asymptotically stable.*

Remark 23. *It is interesting that $H(s)$ in Theorem 6 does not directly depend on $\alpha = 0$. For this reason, if it is possible to find $\gamma \geq 0$ independent of α for all $\alpha \in (0,1]$, then it is possible to take limits in* (5.9)*, that is*

$$1-(1-\gamma s)H(s) = \lim_{\alpha \to 0^+} 1-(1-\gamma s)(1-\alpha)H(s)$$

to conclude stability for all $\alpha \in (0,1]$. This will be illustrated in the examples.

Satisfaction of the conditions in Theorem 6 have been shown to imply satisfaction of the conditions in Lemma 12. The converse is also true, as shown in the next theorem.

Theorem 7. *Let* $\alpha \in (0,1]$, $\gamma \geq 0$, *and consider the linear time-invariant system G and its associated transfer functions* G_α *and H define in* (5.6) *and* (5.8). *The following statements are equivalent:*

*1) *G_α *is asymptotically stable and*

$$1 + (1+\gamma s)(1-\alpha)G_\alpha(s) \tag{5.13}$$

is SPR.

2) H is asymptotically stable and

$$1 - (1-\gamma s)(1-\alpha)H(s) \tag{5.14}$$

is SPR.

Proof. The implication 2) $\implies$ 1) is given by Theorem 6. In order to establish that 1) $\implies$ 2) assume that G_α is asymptotically stable and

$$\frac{1}{1-\alpha} + (1+\gamma s)G_\alpha(s)$$

is strictly positive real. Expression (5.13) being SPR implies that

$$\frac{1}{1-\alpha} + \mathrm{Re}\{G_\alpha(j\omega)\} - \gamma\omega\,\mathrm{Im}\{G_\alpha(j\omega)\} > 0 \tag{5.15}$$

for all $\omega > 0$. For any ω such that $\mathrm{Im}\{G_\alpha(j\omega)\} = 0$, it is true that

$$\mathrm{Re}\{G_\alpha(j\omega)\} > -\frac{1}{1-\alpha},$$

This indicates that the Nyquist plot of $G_\alpha(j\omega)$ only intersects the real axis to the right of the

point $-1/(1-\alpha)$. Because that G_α is asymptotically stable, it does not have any imaginary poles, therefore the Nyquist plot of G_α never encircles $-1/(1-\alpha)$. Thus, by the Nyquist stability criterion [DO17],

$$\frac{G_\alpha(s)}{1+(1-\alpha)G_\alpha(s)} = \frac{G_\alpha(s)}{1-\alpha G_\alpha(s)+G_\alpha(s)} = \frac{G(s)}{1+G(s)} = H(s)$$

is asymptotically stable.

Next, define

$$X(s) = (1-\alpha)\,\mathrm{Re}\{G_\alpha(s)\}, \qquad Y(s) = (1-\alpha)\,\mathrm{Im}\{G_\alpha(s)\},$$

such that (5.15) can be written as

$$1+X(j\omega)-\gamma\omega Y(j\omega) > 0 \tag{5.16}$$

and also note that

$$(1+X(j\omega))^2+Y(j\omega)^2 > 0 \tag{5.17}$$

Divide (5.16) by (5.17) to arrive at

$$\mathrm{Re}\{W(j\omega)\} = \frac{1+X(j\omega)-\gamma\omega Y(j\omega)}{(1+X(j\omega))^2+Y(j\omega)^2} > 0$$

in which

$$W(s) = \frac{(1-\gamma s)(1+X(s)-jY(s))}{(1+X(s)+jY(s))(1+X(s)-jY(s))}+\gamma s$$

is SPR. Note that

$$\begin{aligned} W(s) &= \frac{1-\gamma s}{1+X(s)+jY(s)} + \gamma s \\ &= \frac{1+X(s)+jY(s)-(1-\gamma s)(X(s)+jY(s))}{1+X(s)+jY(s)} \\ &= 1-(1-\gamma s)\frac{X(s)+jY(s)}{1+X(s)+jY(s)} \\ &= 1-(1-\gamma s)(1-\alpha)\frac{G_\alpha(s)}{1+(1-\alpha)G_\alpha(s)} \\ &= 1-(1-\gamma s)(1-\alpha)H(s) \end{aligned}$$

such that since $0 < \alpha < 1$,

$$1-(1-\gamma s)(1-\alpha)H(s)$$

is also SPR. □

5.4 Examples

To illustrate Theorems 6 and 7 and its remarks, examples covering virtually all analytical results in the literature will be revisited in this section.

Example 6 (Second-order Type-I PLL with one zero)**.** *Consider the second order PLL example from [Abr89], in which the loop transfer-function is*

$$G(s) = K\frac{s+b}{s(s+a)}, \qquad a,b,K > 0$$

and the closed-loop transfer function

$$H(s) = K\frac{s+b}{s^2+(a+K)s+bK}$$

is asymptotically stable for any choice of $a, b, K > 0$.

In this example, condition (5.9) *is*

$$\mathrm{Re}\{H(j\omega)\} + \gamma\omega\,\mathrm{Im}\{H(j\omega)\} = K\frac{b^2K + \omega^2(K+a-b) - \gamma\omega^2(\omega^2+ab)}{(\omega^2-bK)^2+\omega^2(a+K)^2} < \frac{1}{1-\alpha}$$

for all $\omega > 0$. *Subtracting one from both sides and inverting the sign of the inequality one obtains*

$$\omega^2\frac{(1+K\gamma)\omega^2 + (a^2+aK-bK+\gamma abK)}{(\omega^2-bK)^2+\omega^2(a+K)^2} > -\frac{\alpha}{1-\alpha}.$$

It can be seen that if

$$\gamma > \frac{bK-a^2-aK}{abK} \tag{5.18}$$

then

$$\omega^2\frac{(1+K\gamma)\omega^2 + (a^2+aK-bK+\gamma abK)}{(\omega^2-b)^2+\omega^2(a+1)^2} \geq 0 > -\frac{\alpha}{1-\alpha}.$$

for all $\alpha \in (0,1)$ *and* $\omega \in \mathbb{R}$. *Note that* γ *is independent of* α *so the conclusion can be extended to all* $\alpha \in (0,1]$.

The Popov plot of $H(j\omega)$ *is shown in Figure 5.6, where the dashed curve is*

$$(\mathrm{Re}\{H(j\omega)\}, \omega\,\mathrm{Im}\{H(j\omega)\})$$

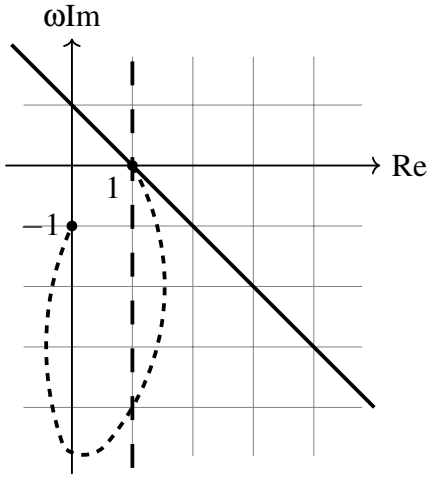

Figure 5.6: Popov plot $a = K = 1, b = 10$

and the solid straight line is

$$\omega \mathrm{Im}\{H(j\omega)\} = -\frac{1}{\gamma}\mathrm{Re}\{H(j\omega)\} + \frac{1}{\gamma}.$$

If the dashed curve lies below the solid straight line, the conditions in Theorem 6 are satisfied.

Note that if $a \geq b$, then the right hand side of (5.18) *is negative so that the Theorem is satisfied for $\gamma = 0$, that is the Circle criterion. If $b > a$, then the Circle criterion fails to prove stability as illustrated by the dashed vertical line in Figure 5.6, where $a = K = 1$, $b = 10$.*

Note that PLL stability was proved in [Abr89] for the case $b > a$ using a Popov-type Lyapunov function but the analysis required the use of LaSalle's invariance principle. Our approach can handle all range of a and b without the need to invoke LaSalle's invariance principle.

In the previous example, Theorem 6 was valid for all $\alpha \in (0, 1]$ and the choice of γ turned out to be independent of α. This is not always the case, as we shall see in the next examples.

Example 7 (Second-order Type-II PLL)**.** *Consider the following second-order PLL with two*

integrators (Type-II),

$$G(s) = \frac{K(s+b)}{s^2}, \qquad b, K > 0. \tag{5.19}$$

The closed-loop transfer function

$$H(s) = \tilde{H}(s/b), \qquad \tilde{H}(s) = \tilde{K}\frac{s+1}{s^2+\tilde{K}s+\tilde{K}}, \qquad \tilde{K} = K/b,$$

is asymptotically stable for any $\tilde{K} > 0$, that is for any $b, K > 0$. Therefore it is enough to verify whether

$$\frac{1}{1-\alpha} - \mathrm{Re}\{\tilde{H}(j\omega)\} - \gamma\omega\,\mathrm{Im}\{\tilde{H}(j\omega)\} > 0,$$

for all $\omega > 0$, which is equivalent to

$$\frac{1}{1-\alpha}\frac{(1+\tilde{K}\gamma(1-\alpha))\,\omega^4 + \tilde{K}(\tilde{K}\alpha - 1\alpha - 1)\omega^2 + \tilde{K}^2\alpha}{(\omega^2-\tilde{K})^2 + \tilde{K}^2\omega^2} > 0$$

for all $\omega > 0$. Because the denominator is positive, the above condition will be true if

$$(1+\tilde{K}\gamma(1-\alpha))\,\omega^4 + \tilde{K}(\tilde{K}\alpha - 1\alpha - 1)\omega^2 + \tilde{K}^2\alpha > 0$$

for all $\omega > 0$. The above quartic polynomial is quadratic in ω^2 so that it is enough to pick

$$\gamma > \frac{1+\alpha^2(1-\tilde{K})^2 - 2\alpha(1+\tilde{K})}{4\tilde{K}\alpha(1-\alpha)}.$$

for the above condition to hold for all $\omega > 0$ and any $\alpha \in (0,1)$. Even though a value of γ exists for any $\alpha \in (0,1)$, it is not possible to select γ independently of α as in Example 1. The Popov plot of H provides the intuition behind deriving the value of α and a choice of γ as shown in

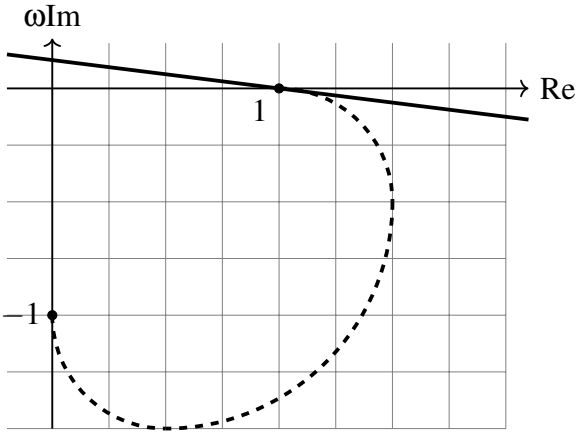

5.7(a) Popov plot $\tilde{K} = 1$. The slope of the solid straight line equals to $-1/\gamma$

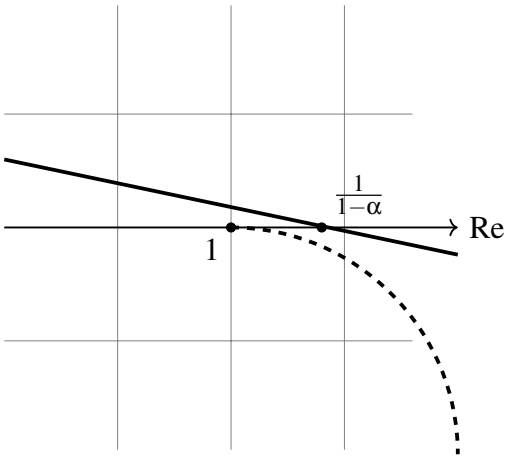

5.7(b) Zoom in to the intersection area.

Figure 5.7

Figure 5.7.

In the previous two examples, it was possible to prove PLL stability for any $\alpha \in (0,1]$. Those were PLLs of type I and II. For PLL of type III and higher it is generally not be possible to prove PLL stability for all $\alpha \in (0,1]$, as illustrated by the next example.

Example 8 (Third-order Type-II PLL)**.** *Consider the third-order PLL from [Abr89],*

$$G(s) = K\frac{s^2 + b_1 s + b_0}{s^2(s + a_1)}, \qquad a_1, b_0, b_1, K > 0 \tag{5.20}$$

The closed-loop transfer function is

$$H(s) = \frac{K(s^2 + b_1 s + b_0)}{s^3 + (a_1 + K)s^2 + b_1 K s + b_0 K},$$

which, by Routh-Hurwitz stability criterion [Oga10], is asymptotically stable if $a_1 + K > 0$*,* $b_0 K > 0$*,* $(a_1 + K)b_1 > b_0$*. The first two conditions are trivially satisfied and H is asymptotically*

stable if

$$K > \frac{b_0}{b_1} - a_1.$$

For PLL stability, evaluate

$$\begin{aligned}
\mathrm{Re}\{H(j\omega)\} &= K\frac{(a_1 - b_1 + K)\omega^4 + (b_1^2 K - b_0(a_1 + 2K))\omega^2 + b_0^2 K}{((a_1 + K)\omega^2 - b_0 K)^2 + \omega^2(\omega^2 - b_1 K)^2}, \\
\mathrm{Im}\{H(j\omega)\} &= -\frac{K\omega^3(\omega^2 - b_0 + a_1 b_1)}{((a_1 + K)\omega^2 - b_0 K)^2 + \omega^2(\omega^2 - b_1 K)^2},
\end{aligned}$$

for which the denominator, $\left((a_1 + K)\omega^2 - b_0 K\right)^2 + \omega^2(\omega^2 - b_1 K)^2 > 0$*, because* $b_0 K$ *and* $b_1 K$ *are both positive.*

If $b_0 \leq a_1 b_1$ *the imaginary part of* $\omega H(j\omega)$ *is non-positive for all* ω *and it is equal to zero only at* $\omega = 0$*, as shown in Figure 5.85.8(a). In this case, as suggested by Figure 5.85.8(a), it is possible to select* $\alpha > 0$ *arbitrarily close to zero. As in Example 7, a corresponding value of* γ *is available for any such* α*, but a formula is not immediately at hand. We will prove this fact indirectly using the following separating hyperplane argument. Consider the 2- dimensional curve*

$$\mathcal{H} = \left\{x \in \mathbb{R}^2 \mid x = (\mathrm{Re}\{H(j\omega)\}, \omega\,\mathrm{Im}\{H(j\omega)\})\right\}$$

and the convex set obtained by taking its convex hull [BV04], $\mathrm{conv}\,\mathcal{H}$*. The convex hull of* $\mathcal{X}$*, denoted* $\mathrm{conv}\,\mathcal{X}$*, is the smallest convex set in which* $\mathcal{X}$ *is contained.*

Consider also the convex set

$$\mathcal{G} = \mathrm{conv}\,\{(1/(1-\alpha), 0), (1, 1)\}$$

which is a segment of a line. Because $H(j0) = 1$ *is the only point such that* $\mathrm{Im}\{H(j\omega)\} = 0$ *and*

$\omega \mathrm{Im}\{H(j\omega)\} < 0$ *for all* $\omega \neq 0$*, it follows that*

$$\mathcal{G} \cap \mathrm{conv}\, \mathcal{H} = \emptyset$$

for all $\alpha \in (0,1)$*. Therefore, by the Separating Hyperplane Theorem [BV04], there exist a and b such that*

$$a^T x < b, \qquad a^T y > b, \qquad x \in \mathrm{conv}\, \mathcal{H}, \qquad y \in \mathcal{G}.$$

If $a = (a_1, a_2)$*, then letting* $x = (1,0) \in \mathrm{conv}\, \mathcal{H}$*,* $y = (1/(1-\alpha), 0) \in \mathcal{G}$ *one concludes that*

$$b(1-\alpha) < a_1 < b \qquad \Longrightarrow \qquad a_1 > 0, \quad b > 0, \quad 1 < \frac{b}{a_1} < \frac{1}{1-\alpha},$$

and letting $y = (1,1) \in \mathcal{G}$

$$a_2 > b - a_1 > 0.$$

Therefore for any

$$x = (\mathrm{Re}\{H(j\omega)\}, \omega \mathrm{Im}\{H(j\omega)) \in \mathcal{H} \subseteq \mathrm{conv}\, \mathcal{H}$$

it must be true that

$$\mathrm{Re}\{H(j\omega)\} + \frac{a_2}{a_1} \omega \mathrm{Im}\{H(j\omega) < \frac{b}{a_1} < \frac{1}{1-\alpha}$$

for all $\omega > 0$*. This means that there exists* $\gamma = a_2/a_1 > 0$ *such that* (5.10) *is true so that Theorem 6 holds for any* $\alpha \in (0,1)$*.*

If $b_0 - a_1 b_1 > 0$, H is the asymptotically stable only if

$$K > \frac{b_0}{b_1} - a_1 > 0.$$

As shown in Figure 5.85.8(b),

$$H(j0) = 1, \qquad H(j\sqrt{b_0 - a_1 b_1}) = \frac{K}{K - (\frac{b_0}{b_1} - a_1)} > 1,$$

are the only two points for which $\mathrm{Im}\{H(j\omega\} = 0$. *Therefore, if*

$$\bar{\alpha} = \frac{1}{K}\left(\frac{b_0}{b_1} - a_1\right). \tag{5.21}$$

then it is necessary that $\alpha > \bar{\alpha}$ *so that*

$$\frac{1}{1-\alpha} > H(j\sqrt{b_0 - a_1 b_1}) = \frac{K}{K - (\frac{b_0}{b_1} - a_1)}$$

for PLL stability.

Figure 5.85.8(b) suggests that, for any $\alpha > \bar{\alpha}$, *a possible choice of* γ *is the inverse of the slope of the tangent to the curve* $(\mathrm{Re}\{H(j\omega)\}, \omega\,\mathrm{Im}\{H(j\omega)\})$ *at* $(\bar{\alpha}, 0)$, *that is at* $\omega = \sqrt{b_0 - a_1 b_1}$. *In other words*

$$-\frac{1}{\gamma} = \frac{\frac{d}{d\omega}(\omega\,\mathrm{Im}\{H(j\omega)\})}{\frac{d}{d\omega}(\mathrm{Re}\{H(j\omega)\})}\Big|_{\omega=\sqrt{b_0 - a_1 b_1}} = -\frac{(b_0 - a_1 b_1)^2}{a_1 b_0 + b_0 b_1 - a_1 b_1^2}.$$

Note that

$$\gamma = \bar{\gamma} = \frac{a_1 b_0 + b_1(b_0 - a_1 b_1)}{(b_0 - a_1 b_1)^2} > 0$$

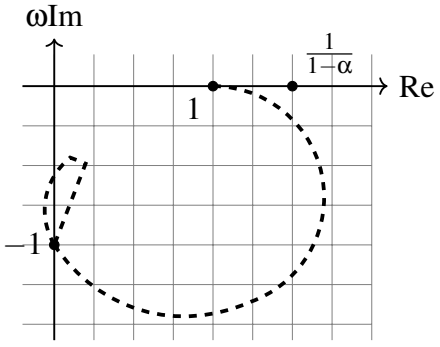

5.8(a) Popov plot of H, $a_1 = 2$

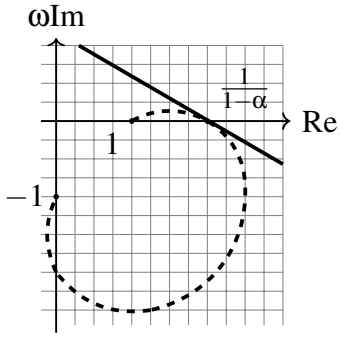

5.8(b) Popov plot of H, $a_1 = 0.5$

Figure 5.8: Third-order type-II PLL, $b_0 = b_1 = K = 1$.

is independent of K. Furthermore for any $\alpha > \bar{\alpha}$ *given by* (5.21) *then*

$$\frac{1}{1-\alpha} - \mathrm{Re}\{H(j\omega)\} - \bar{\gamma}\omega\,\mathrm{Im}\{H(j\omega)\} > \frac{K\left(\omega^2 - (b_0 - a_1 b_1)\right)^2 \left(\omega^2\left(b_1^2 K(b_0 - a_1 b_1) + b_1 K - (b_0 - a_1 b_1)\right) + b_0^2 K(b_0 - a_1 b_1)\right)}{(b_0 - a_1 b_1)^2 \left(b_1 K - (b_0 - a_1 b_1)\right)\left((a_1 + K)\omega^2 - b_0 K\right) + \omega^2(\omega^2 - b_1 K))} \geq 0,$$

for all ω *because* $Kb_1 > b_0 - a_1 b_1 > 0$ *and* $a_1, b_0, b_1, K > 0$. *This inequality is equivalent to* (2.3).

This example was considered in [Abr89], in which a Lyapunov and LaSalle's invariance principal argument was able to show PLL stability under the assumption that $b_0 - (b_1 + a_1)a_1 > 0$. *This is a subset of our first case condition* $b_0 \geq a_1 b_1$. *The more complicated case* $b_0 < a_1 b_1$ *was not considered in [Abr89].*

Example 7 is the first occasion in which a nonzero lower bound on α is required, in other words, that a full locking range is not possible. Unfortunately, this seems to be the norm for any PLL of type higher or equal than 3, as discussed in the next section.

5.5 Higher-type PLL stability

PLL systems with type higher than one are desirable in many applications. One example is the use of a type-III PLL in mobile coherent receivers to compensate for Doppler effects. Unfortunately, it is possible to show that the value of α in Theorem 6 will always be bounded away from zero for PLLs with type higher or equal to 3. This results is the subject of the next lemma. In this lemma $G'(j\omega)$ denotes the derivative of $G(j\omega)$ with respect to ω.

Lemma 13. *Consider the feedback connection between the nonlinear function* $\psi \in [\alpha, 1]$, $\alpha \in (0, 1]$, *with the linear time-invariant system with a strictly proper transfer-function* $G(s)$ *of the form,*

$$G(s) = s^{-r} K \Gamma(s), \qquad \Gamma(0) = 1,$$

in which $r \geq 3$ *and* $\Gamma(s)$ *is asymptotically stable. Assume that Theorem 6 holds. Then there exists*

$$\omega_p = \arg\max_k \{\mathrm{Re}\{G(j\omega_k)\} : \quad \mathrm{Im}\{G(j\omega_k)\} = 0, \quad \mathrm{Re}\{G(j\omega_k)\} < -1\} \tag{5.22}$$

such that

$$\alpha > \beta^{-1}, \qquad \beta = -\mathrm{Re}\{G(j\omega_p)\} > 1. \tag{5.23}$$

Furthermore, $z_p = (\beta/(\beta-1), 0)$ *is the point at the intersection of the curve*

$$(\mathrm{Re}\{H(j\omega)\}, \omega \mathrm{Im}\{H(j\omega)\})$$

and the real axis with largest real part. The slope of the line tangent to the curve at z_p is

$$-\frac{1}{\gamma_p} = \frac{\omega_p \operatorname{Im}\{G'(j\omega_p)\}}{\operatorname{Re}\{G'(j\omega_p)\}} = \omega_p \tan \angle G'(j\omega_p)$$

which is independent of the static gain K and

$$G'(j\omega) := \frac{d}{d\omega} G(j\omega).$$

Proof. Assume that Theorem 6 holds for some $0 < \alpha \leq 1$ and $\gamma \geq 0$ so that $H(s)$ is asymptotically stable and consider the Nyquist plot of $G(s)$. Because $G(s)$ has $r \geq 3$ integrators and $\Gamma(s)$ is asymptotically stable, the Nyquist plot has one arc at infinity that encircles the point -1 at least 1 time in the counter-clockwise direction. See illustration in Example 9. According to the Nyquist stability criterion, the finite part of the Nyquist plot of G must therefore encircle the point -1 at least one time in the clockwise direction. In other words, $G(j\omega)$ intersects the negative real axis at least once to the left of the point -1, which ensures the existence of ω_p and $\beta > 1$ as in (5.22) and (5.23).

Because $\operatorname{Im}\{G(j\omega)\} = 0$ if and only if $\operatorname{Im}\{H(j\omega)\} = 0$, and

$$\frac{1}{1-\alpha} - \operatorname{Re}\{H(j\omega)\} - \gamma\omega \operatorname{Im}\{H(j\omega)\} > 0$$

for all $\omega > 0$, it is true that

$$\frac{1}{1-\alpha} > \operatorname{Re}\{H(j\omega_p)\} = \frac{\operatorname{Re}\{G(j\omega_p)\}}{1+\operatorname{Re}\{G(j\omega_p)\}} > 0$$

at $\omega = \omega_p$ as in (5.22). The last inequality follows from the fact that $\beta = -\operatorname{Re}\{G(j\omega_p)\} > 1$. In other words, $\alpha > \beta^{-1} > 0$.

The next goal is to evaluate

$$-\frac{1}{\gamma_p} = \left.\frac{\frac{d}{d\omega}(\omega \mathrm{Im}\{H(j\omega)\})}{\frac{d}{d\omega}(\mathrm{Re}\{H(j\omega)\})}\right|_{\omega=\omega_p} = \frac{\omega_p \mathrm{Im}\{H'(j\omega_p)\}}{\mathrm{Re}\{H'(j\omega_p)\}},$$

Note that because

$$H'(j\omega) = \frac{(1+G(j\omega))G'(j\omega) - G(j\omega)G'(j\omega_p)}{(1+G(j\omega))^2} = \frac{G'(j\omega)}{(1+G(j\omega))^2}$$

and $\mathrm{Im}\{H(j\omega_p)\} = \mathrm{Im}\{G(j\omega_p)\} = 0$ then $(1+G(j\omega_p))$ is real and

$$-\frac{1}{\gamma_p} = \frac{\omega_p \mathrm{Im}\{G'(j\omega_p)\}}{\mathrm{Re}\{G'(j\omega_p)\}} = \omega_p \tan\angle G'(j\omega_p).$$

which is independent of the static gain K because K is a common factor multiplied on both $\mathrm{Im}\{G'(j\omega_p)\}$ and $\mathrm{Re}\{G'(j\omega_p)\}$. □

Remark 24. *Note that* β *in Lemma 13 is the system's gain margin* $GM = 20\log_{10}\beta^{-1} < 0$. *Interestingly, the reference [GMFG13] explicitly utilizes the gain margin of a type-III PLL as a critical parameters in analyzing the dynamics and stability of type-III PLL response. Lemma 13 suggests that the gain margin is a critical parameter in the stability analysis of PLLs of type higher or equal than three.*

Example 9 (Third-order Type-III PLL)**.** *Consider the following third-order type-III PLL with normalized zeros,*

$$G(s) = K\frac{(s+b)^2}{s^3}, \qquad \tilde{G}(s) = \tilde{K}\frac{(s+1)^2}{s^3}, \qquad K, b > 0 \tag{5.24}$$

for which the closed-loop transfer function is

$$H(s) = \tilde{H}(s/b), \qquad \tilde{H}(s) = \frac{\tilde{K}(s+1)^2}{s^3 + \tilde{K}(s^2+2s+1)}, \qquad \tilde{K} = \frac{K}{b}.$$

Using the Nyquist stability criterion, see Figure 5.95.9(a), $H(s)$ is asymptotically stable for any $K > 1/2$. For PLL stability one needs to verify whether

$$\frac{1}{1-\alpha} - \mathrm{Re}\{\tilde{H}(j\omega)\} - \gamma\omega\,\mathrm{Im}\{H(j\omega)\} > 0,$$

for all $\omega > 0$, in which

$$\mathrm{Re}\{\tilde{H}(j\omega)\} = \frac{\tilde{K}^2(1+\omega^2)^2 - 2\tilde{K}\omega^4}{\omega^2(\omega^2-2\tilde{K})^2 + \tilde{K}^2(\omega^2-1)^2},$$
$$\omega\,\mathrm{Im}\{\tilde{H}(j\omega)\} = -\frac{\tilde{K}\omega^4(\omega^2-1)}{\omega^2(\omega^2-2\tilde{K})^2 + \tilde{K}^2(\omega^2-1)^2}.$$

Note that $\omega\,\mathrm{Im}\{\tilde{H}(j\omega)\} = 0$ only at $\omega = 0$ and $\omega = 1$, and that

$$\tilde{H}(j1) = \frac{\tilde{K}}{\tilde{K}-1/2} > 1 = H(j0).$$

In order for the curve $(\mathrm{Re}\{\tilde{H}(j\omega)\}, \omega\,\mathrm{Im}\{\tilde{H}(j\omega)\})$ to lie below the Popov line, the rightmost intersection point, $H(j1)$, must be on the left of $1/(1-\alpha)$, as shown in Figure 5.95.9(b). In other words

$$\frac{1}{1-\alpha} > \frac{\tilde{K}}{\tilde{K}-1/2} \quad \Rightarrow \quad \alpha > \frac{1}{2\tilde{K}} > 0$$

As predicted by Lemma 13, α is bounded away from zero for all finite $\tilde{K}$. To verify the second part of Lemma 13, evaluate the expression

$$-\frac{1}{\gamma_p} = \frac{\omega_p\,\mathrm{Im}\{\tilde{G}'(j\omega_p)\}}{\mathrm{Re}\{\tilde{G}'(j\omega_p)\}} = -\frac{1}{2}$$

which is independent of the static gain K.

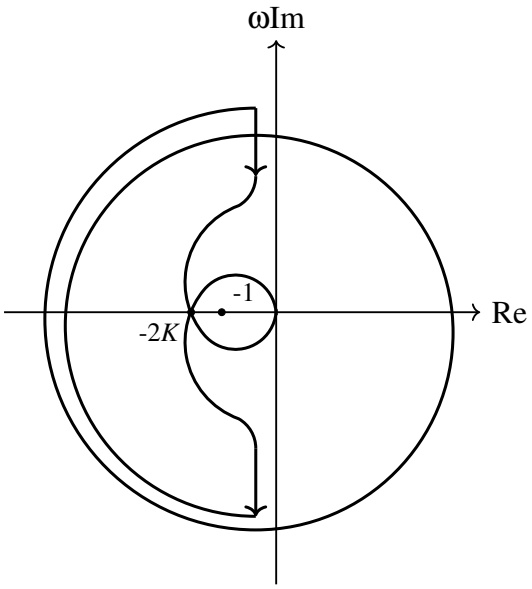

5.9(a) Nyquist plot of $\tilde{G}$

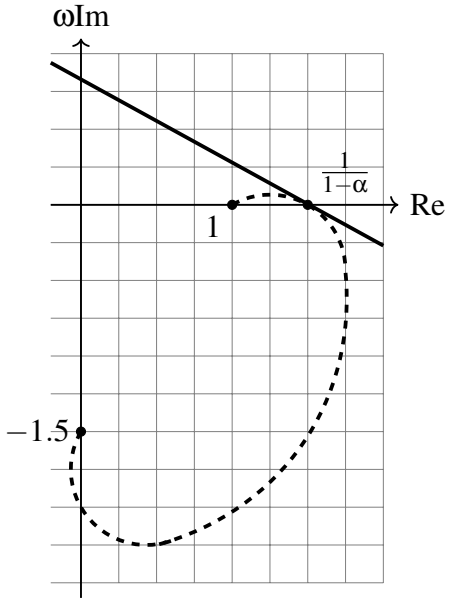

5.9(b) Popov plot of $\tilde{H}$

Figure 5.9: Third-order type-III PLL from Example 9, $K = 1$

In this example, the constant value of $\gamma_p = 2$ calculated above is enough to verify that

$$\frac{\tilde{K}}{\tilde{K}-1/2} - \mathrm{Re}\{\tilde{H}(j\omega)\} - 2\omega\,\mathrm{Im}\{\tilde{H}(j\omega)\} = \frac{2\tilde{K}^2(\omega^2-1)^2(4\omega^2+1)}{(2\tilde{K}-1)\left(\omega^2(\omega^2-2\tilde{K})^2+\tilde{K}^2(\omega^2-1)^2\right)} > 0$$

for all $\tilde{K} > 1/2$.

5.6 Simulations

The analysis in chapter is based on the phase model of PLL, as in Figure 5.25.2(b). As discussed in Section 5.1, the phase model is a simplified model of the PLL in which the high-frequency components generated at the phase detector are ignored. In order to validate the proposed stability analysis developed in this chapter, simulations of the complete PLL systems, as in Figure 5.10, will be provided in this section. A Matlab Simulink model of the system in Figure 5.10 will be used for simulation. The stability and performance of the PLL is evaluated

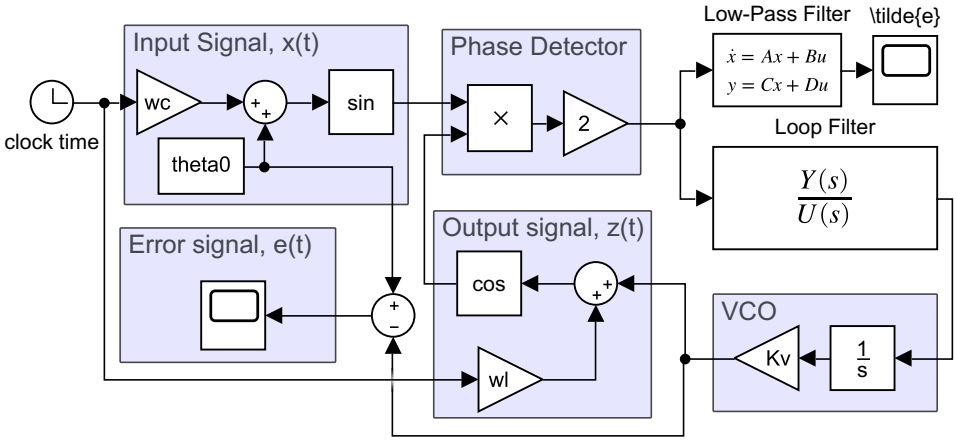

Figure 5.10: Simulation block diagram

with respect to phase error signal, $e(t)$, which is obtained as shown in Figure 5.10. In the following simulations, the carrier and VCO frequencies are set as $\omega_c = \omega_\ell = 10^4$ rad/s and the VCO gain $K_v = 1$.

5.6.1 2nd-order Type-II PLL (Example 7)

The second-order type-II PLL with loop filter

$$F(s) = \frac{Y(s)}{U(s)} = \frac{K(s+b)}{s}$$

from Example 7 is simulated with $K = b = 1$.

It is predicted that the system is able to achieve locking in the range $(-\pi, \pi)$. In order to validate this prediction we selected an initial phase $e(0) = \theta_0 = 3.14 < \pi$. As shown in Figure 5.11, $e(t)$ converges to 0, at which point the loop is successfully locked. One could further tune the gain K in the loop-filter to adjust the settling time if wanted.

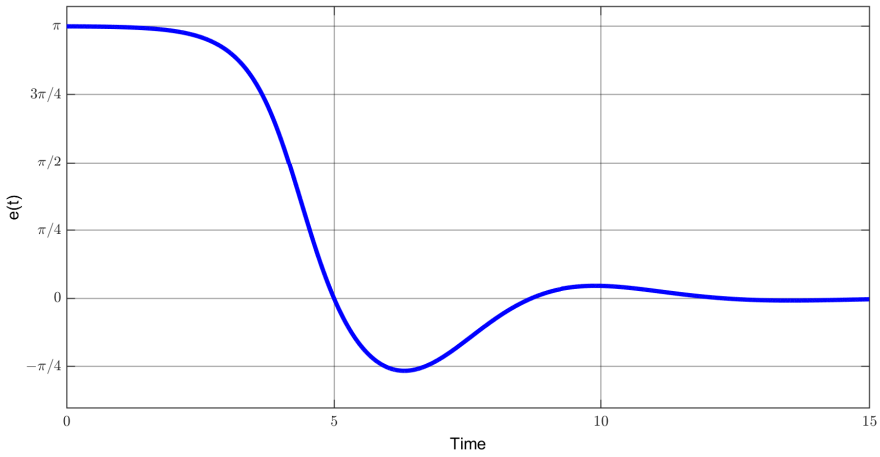

Figure 5.11: Second-order type-II PLL from Example 7, $K = b = 1$

5.6.2 Third-order Type-II PLL (Example 8, $b_0 \leq a_1 b_1$)

The second-order type-II PLL with loop filter

$$F(s) = \frac{Y(s)}{U(s)} = \frac{K(s^2 + b_1 s + b_0)}{s(s + a_1)}$$

from Example 8 is simulated with $K = 10$, $b_0 = b_1 = 1$, and $a_1 = 2$. In this case, $b_0 \leq a_1 b_1$.

It is predicted that the system is able to achieve locking in the range $(-\pi, \pi)$. An initial phase $e(0) = \theta_0 = 3.14 \neq \pi$ is selected. As shown in Figure 5.12, $e(t)$ converges to 0, at which point the loop is successfully locked.

5.6.3 3rd-order Type-II PLL (Example 8, $b_0 > a_1 b_1$)

This is the same system as before, this time with $K = 10$, $b_0 = b_1 = 1$, and $a_1 = 0.5$, such that $b_0 > a_1 b_1$.

It is predicted that the system is able to achieve locking in the range $(-\text{sinc}\{\bar{\alpha}\}, \text{sinc}\{\bar{\alpha}\})$,

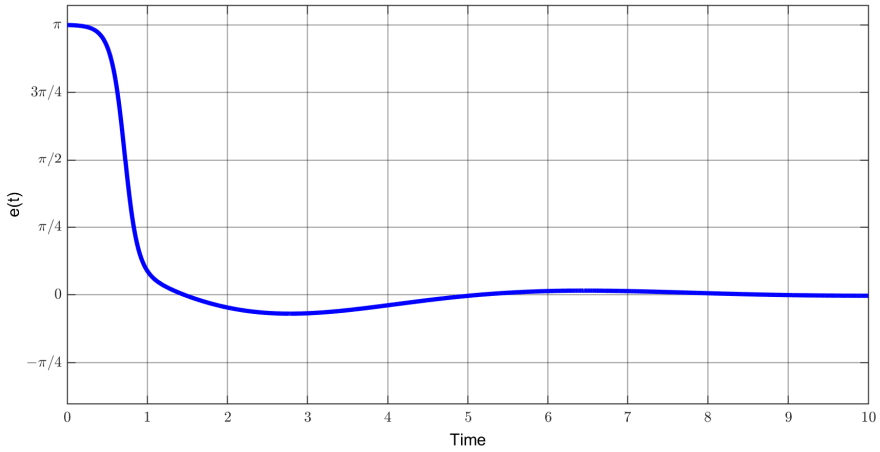

Figure 5.12: Third-order type-II PLL from Example 8, $b_0 \leq a_1 b_1$

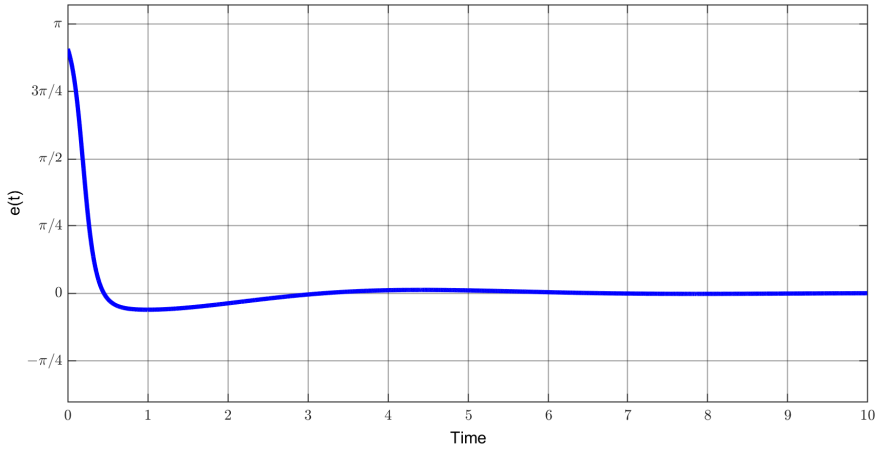

Figure 5.13: 3rd-order type-II PLL from Example 8, $b_0 > a_1 b_1$

in which

$$\bar{\alpha} = \frac{1}{K}\left(\frac{b_0}{b_1} - a_1\right) = 0.05.$$

An initial phase $e(0) = \theta_0 = \text{sinc}^{-1}\{\bar{\alpha}\} \approx 2.85$ is used for simulation. As shown in Figure 5.12, $e(t)$ converges to 0, at which point the loop is successfully locked.

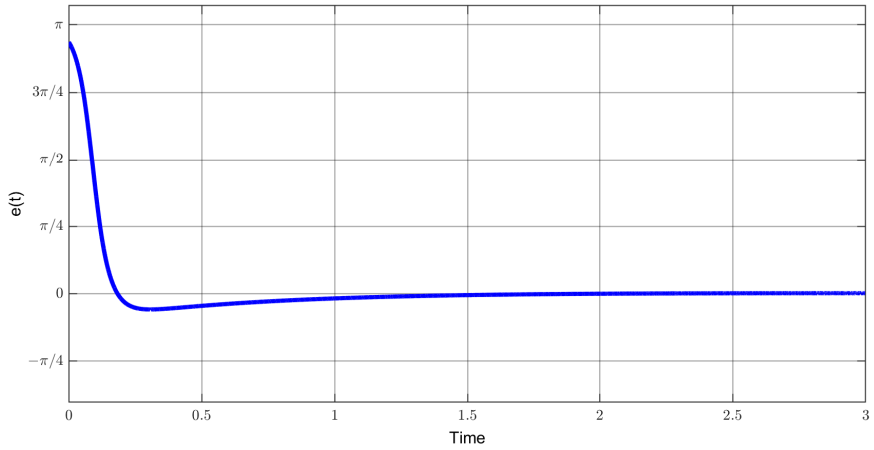

Figure 5.14: Third-order type-III PLL from Example 9, $K = 25,\ b = 1$

5.6.4 3rd-order Type-III PLL (Example 9)

The third-order type-III PLL with loop filter

$$F(s) = \frac{Y(s)}{U(s)} = \frac{K(s+b)^2}{s^2},$$

from Example 9 is simulated with $K = 25$, $b = 1$.

It is predicted that the system is able to achieve locking in the range $(-\text{sinc}\{\alpha\}, \text{sinc}\{\alpha\})$, in which $\alpha = 1/(2K) = 0.02$. An initial phase $e(0) = \theta_0 = \text{sinc}^{-1}\{0.02\} \approx 2.94$ is used for simulation. The result is shown in Figure 5.14, where $e(t)$ converges to 0, at which point the loop is successfully locked.

5.6.5 3rd-order Type-III PLL, frequency mismatch (Example 9)

The main motivations for using PLLs of higher type is to be able to lock even in the presence of frequency mismatches. In order to illustrate that, the same third-order type-III PLL from Example 9 is simulated with $\omega_\ell = \omega_c + 10$ rad/s while the other parameters, including the initial phase $e(0) = \theta_0 \approx 2.94$, remain the same. It is predicted that $e(t) = \theta_0 - \phi$ converges to $(\omega_\ell - \omega_c)t = 10t$, as seen in Figure 5.15. In order to see that the loop is indeed locked, the

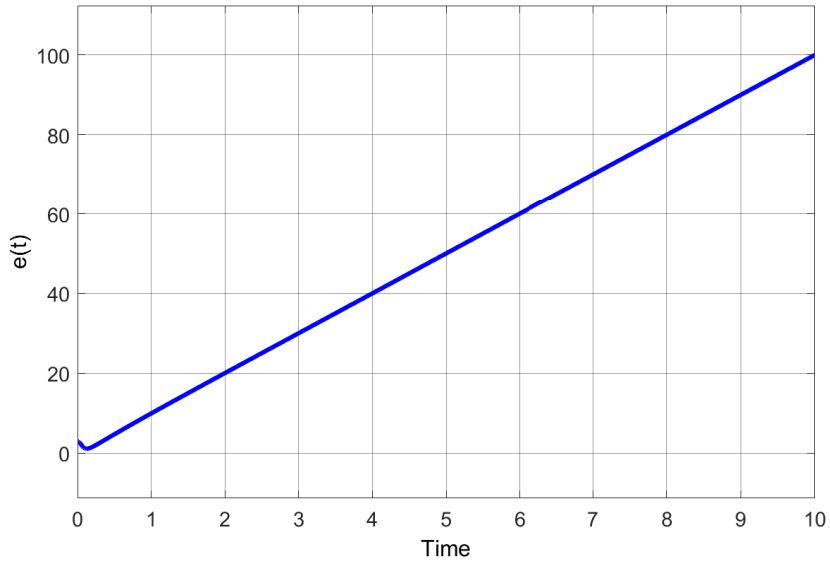

Figure 5.15: Example 4 with frequency mismatch. Signal $e(t)$ converged to $10t$

low-pass component of the signal $\tilde{e}(t)$ from (5.4), i.e. $\sin((\omega_c - \omega_\ell)t + e(t))$, which is predicted to go to zero, is plotted in Figure 5.15. A low-pass filter with cutoff frequency at 100 rad/s is used to produce the low-pass component of $\tilde{e}(t)$, as shown in Figure 5.16.

5.7 Acknowledgment

Chapter 5, in full, is a reprint of the material as it appears in: Chen, Yilong, and Mauricio C. de Oliveira. "Revisiting Stability Analysis of Phase-Locked Loops with the Popov Stability Criterion." IFAC Journal of Systems and Control, (Manuscript Number: IFACSC-D-21-00010). The dissertation author was the primary investigator and author of this material.

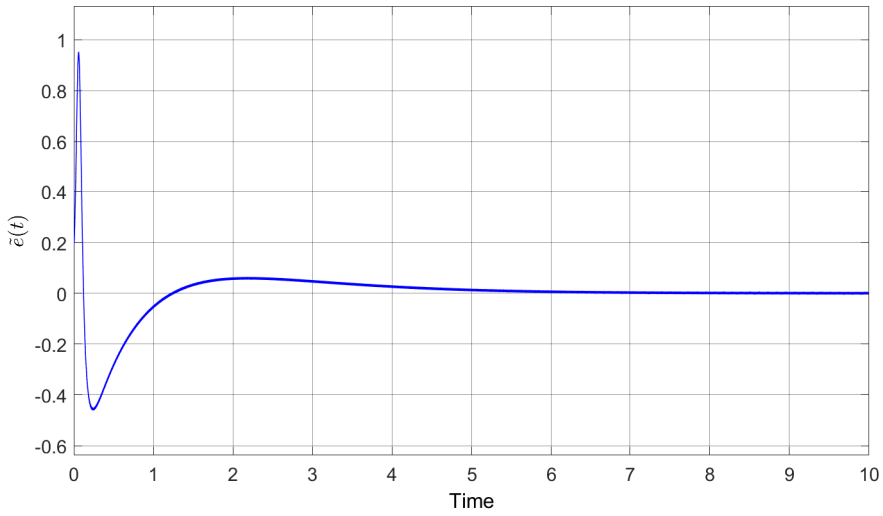

Figure 5.16: Example 4 with frequency mismatch. Low-pass component of $\tilde{e}(t)$ converges to 0.

Bibliography

[Abr89] D. Y. Abramovitch. Lyapunov redesign of analog phase-lock loops. In *1989 American Control Conference*, pages 2684–2689, 1989.

[Abr02a] D. Abramovitch. Phase-locked loops: a control centric tutorial. In *Proceedings of the 2002 American Control Conference (IEEE Cat. No.CH37301)*, volume 1, pages 1–15 vol.1, 2002.

[Abr02b] D. Abramovitch. Phase-locked loops: a control centric tutorial. In *Proceedings of the 2002 American Control Conference (IEEE Cat. No.CH37301)*, volume 1, pages 1–15 vol.1, 2002.

[ACH+18] Zunaib Ali, Nicholas Christofides, Lenos Hadjidemetriou, Elias Kyriakides, Yongheng Yang, and Frede Blaabjerg. Three-phase phase-locked loop synchronization algorithms for grid-connected renewable energy systems: A review. *Renewable and Sustainable Energy Reviews*, 90:434–452, 2018.

[AG64] Mark Aronovich Aizerman and Feliks Rouminovich Gantmacher. *Abosolute Stability of Regulator Systems*. Holden-Day, 1964.

[AG95] Pierre Apkarian and Pascal Gahinet. A convex characterization of gain-scheduled H_∞ controllers. *IEEE Trans. on Automatic Control*, 40(5):853–864, 1995.

[Ahm14] Nur Syazreen Ahmad. A less conservative phaselock criterion with linear matrix inequality condition. In *2014 14th International Conference on Control, Automation and Systems (ICCAS 2014)*, pages 179–183, 2014.

[Ban16] D. Banerjee. *PLL performance, simulation and design (5th Edition*. Dog Ear Publishing, Upper Saddle River, 2016.

[BEGFB94] Stephen Boyd, Laurent El Ghaoui, Eric Feron, and Venkataramanan Balakrishnan. *Linear matrix inequalities in system and control theory*. SIAM, 1994.

[BGKR11] Harm Bart, Israel Gohberg, Marinus A Kaashoek, and André CM Ran. *A state space approach to canonical factorization with applications*, volume 200. Springer Science & Business Media, 2011.

[BV04] Stephen. P. Boyd and Lieven Vandenberghe. *Convex optimization*. Cambridge university press, 2004.

[CHL12] Joaquin Carrasco, William P Heath, and Alexander Lanzon. Factorization of multipliers in passivity and IQC analysis. *Automatica*, 48(5):909–916, 2012.

[CHL13] Joaquin Carrasco, William P Heath, and Alexander Lanzon. Equivalence between classes of multipliers for slope-restricted nonlinearities. *Automatica*, 49(6):1732–1740, 2013.

[CHLL12] Joaquín Carrasco, William P. Heath, Guang Li, and Alexander Lanzon. Comments on "On the Existence of Stable, Causal Multipliers for Systems with Slope-restricted Nonlinearities". *IEEE Transactions on Automatic Control*, 57(9):2422–2428, 2012.

[CTH16] Joaquin Carrasco, Matthew C Turner, and William P Heath. Zames-Falb multipliers for absolute stability: From O' Sheas contribution to convex searches. *European Journal of Control*, 28:1–19, 2016.

[DO17] Maurício C De Oliveira. *Fundamentals of Linear Control*. Cambridge University Press, 2017.

[DV09] Charles A Desoer and Mathukumalli Vidyasagar. *Feedback systems: input-output properties*. SIAM, 2009.

[Eva98] N. Eva Wu. Circle/Popov criteria in phaselock loop design. In *Proceedings of the 1998 American Control Conference. ACC (IEEE Cat. No.98CH36207)*, volume 5, pages 3226–3228 vol.5, 1998.

[Gar05] Floyd M Gardner. *Phaselock techniques*. John Wiley & Sons, 2005.

[GGV18] Saeed Golestan, Josep M Guerrero, and Juan C Vasquez. Steady-state linear kalman filter-based plls for power applications: A second look. *IEEE Transactions on Industrial Electronics*, 65(12):9795–9800, 2018.

[GMF12] Saeed Golestan, Mohammad Monfared, and Francisco D Freijedo. Design-oriented study of advanced synchronous reference frame phase-locked loops. *IEEE Transactions on Power Electronics*, 28(2):765–778, 2012.

[GMFG13] S. Golestan, M. Monfared, F. D. Freijedo, and J. M. Guerrero. Advantages and challenges of a type-3 PLL. *IEEE Transactions on Power Electronics*, 28(11):4985–4997, 2013.

[Gup75] S. C. Gupta. Phase-locked loops. *Proceedings of the IEEE*, 63(2):291–306, 1975.

[HH96] Guan-Chyun Hsieh and James C Hung. Phase-locked loop techniques. a survey. *IEEE Transactions on industrial electronics*, 43(6):609–615, 1996.

[HL01] Tingshu Hu and Zongli Lin. *Control systems with actuator saturation: analysis and design*. Springer Science & Business Media, 2001.

[JDZ91] A. Packard J. Doyle and K. Zhou. Review of LFTs, LMIs, and μ. *Proc. of the 30th IEEE Conf. on Decision and Control*, 2, 1991.

[Jov03] Dragan Jovcic. Phase locked loop system for FACTS. *IEEE transactions on power systems*, 18(3):1116–1124, 2003.

[KG02a] Vikram Kapila and Karolos Grigoriadis. *Actuator saturation control*. CRC Press, 2002.

[KG02b] Hassan. K. Khalil and Jessy. W. Grizzle. *Nonlinear systems*. Prentice hall Upper Saddle River, NJ, 2002.

[KG02c] Hassan K Khalil and Jessy W Grizzle. *Nonlinear systems*, volume 3. Prentice hall Upper Saddle River, NJ, 2002.

[KKEM18] Parag Kanjiya, Vinod Khadkikar, and Mohamed Shawky El Moursi. Adaptive low-pass filter based dc offset removal technique for three-phase plls. *IEEE Transactions on Industrial Electronics*, 65(11):9025–9029, 2018.

[KKL$^+$15] Nikolay V Kuznetsov, Olga A Kuznetsova, Gennady A Leonov, P Neittaanm, Marat V Yuldashev, Renat V Yuldashev, et al. Limitations of the classical phase-locked loop analysis. In *2015 IEEE International Symposium on Circuits and Systems (ISCAS)*, pages 533–536. IEEE, 2015.

[Lei06] F Leibfritz. COMPleib: COnstrained Matrix-optimization Problem library, 2006.

[LKYY15] Gennady A Leonov, Nikolay V Kuznetsov, Marat V Yuldashev, and Renat V Yuldashev. Hold-in, pull-in, and lock-in ranges of pll circuits: rigorous mathematical definitions and limitations of classical theory. *IEEE Transactions on Circuits and Systems I: Regular Papers*, 62(10):2454–2464, 2015.

[Lof04] Johan Lofberg. YALMIP: A toolbox for modeling and optimization in MATLAB. In *IEEE Int. Conference on Robotics and Automation*, pages 284–289. IEEE, 2004.

[mos10] The MOSEK optimization software. *http://www. mosek. com*, 2010.

[Oga10] Katsuhiko Ogata. *Modern control engineering*. Prentice hall, 2010.

[OV15] Alan V Oppenheim and George C Verghese. *Signals, systems and inference*. Pearson, 2015.

[Pap] Ivan Papusha. Bounded-real and positive-real lemmas. `https://ivanpapusha.com/cds270/notes/kyp.pdf`.

[PDP85] E. S. N. Prasad, Gopal K. Dubey, and Srinivasa S. Prabhu. High-Performance DC Motor Drive with Phase-Locked Loop Regulation. *IEEE Transactions on Industry Applications*, IA-21(1):192–201, 1985.

[Pop61] VM Popov. Absolute stability of nonlinear systems of automatic control. *Automation and Remote Control*, 22(8):857–875, 1961.

[RV76] Franco Russo and Lucio Verrazzani. Pull-in behavior of third-order generalized phase-locked loops. *IEEE Transactions on Aerospace and Electronic Systems*, pages 213–218, 1976.

[SGC97] Carsten Scherer, Pascal Gahinet, and Mahmoud Chilali. Multiobjective output-feedback control via LMI optimization. *IEEE Trans. on Automatic Control*, 42(7):896–911, 1997.

[Sha94] Jeff S Shamma. Robust stability with time-varying structured uncertainty. *IEEE Trans. on Aut. Control*, 39(4):714–724, 1994.

[SK00] Michael G Safonov and Vishwesh V Kulkarni. Zames-Falb multipliers for MIMO nonlinearities. *International Journal of Robust and Nonlinear Control*, 10(11-12):1025–1038, 2000.

[TGdSJQ11] Sophie Tarbouriech, Germain Garcia, João Manoel Gomes da Silva Jr, and Isabelle Queinnec. *Stability and stabilization of linear systems with saturating actuators*. Springer Science & Business Media, 2011.

[TSS01] William H Tranter, Donald R Stephens, and Dennis G Sweeney. *Phase-locked Loops and Synchronization Systems: A MATLAB-based Simulation Laboratory*. Prentice Hall, 2001.

[Vid02] Mathukumalli Vidyasagar. *Nonlinear systems analysis*. SIAM, 2002.

[Wu02a] N. E. Wu. Analog phaselock loop design using Popov criterion. In *Proceedings of the 2002 American Control Conference (IEEE Cat. No.CH37301)*, volume 1, pages 16–18 vol.1, 2002.

[Wu02b] N Eva Wu. Analog phaselock loop design using Popov criterion. In *Proceedings of the 2002 American Control Conference (IEEE Cat. No. CH37301)*, volume 1, pages 16–18. IEEE, 2002.

[ZD98] Kemin Zhou and John Comstock Doyle. *Essentials of Robust Control*, volume 104. Prentice Hall, Upper Saddle River, NJ, 1998.

[ZF68] George Zames and P.L. Falb. Stability conditions for systems with monotone and slope-restricted nonlinearities. *SIAM Journal on Control*, 6(1):89–108, 1968.